



AdG ERC OSYRIS



AdG ERC NOQIA



ERC QUAGATUA

EU/AEI MAQS

AvH  
Feodor  
Lynen



Generalitat  
de Catalunya

SGR 1034

CERCA/Program

EU FET-OPTologic



MPG  
MPI  
Garching

QuantumCAT

# Cold atoms meet lattice gauge theory

Fundació Privada  
**CELLEX**

Fundació Mir-Puig

EU

FNP  
Polish Science Foundation

NCN  
Narodowe Centrum Nauki

*Symfonia*



John Templeton  
Foundation



FOQUS,  
FISICATEAMO  
& FIDEUA



**\*iCrea**  
INSTITUCIÓ CATALANA DE  
RECERCA I ESTUDIS AVANÇATS

**Fundació**  
Catalunya - La Pedrera

## PhD ICFO:

Guillem Müller (QI)  
 Nils-Eric G nther (many body)  
 Sergi Juli  (QI, many body)  
 Jessica Almeida (quantum optics)  
 Korbinian Kottman (many body, ML)  
 Mohit Bera (QI, many body)  
 Niccol  Baldelli (many body)  
 Jaume Diez (exp)  
 Tymek Salamon (many body)  
 Anna Dawid (ML, quantum chemistry)  
 Borja Requena (ML)  
 Joana Faixanet (ML)  
 Katerina Gratsea (quantum optics, ML)  
 David Ciraqui Garc a (industrial, ML)  
 Guillem M ller (QI)  
 Gabriel Fern ndez (ML, atto)  
 Philipp Stammer (atto)

## ICFO - Quantum Optics Theory

## Postdocs ICFO:

Gorka Mu oz (Brownian)  
 Daniel Gonz lez (many body)  
 Albert Aloy (QI)  
 Alexandre Dauphin (many body, atto)  
 Tobias Grass (all)  
 Utso Bhattacharya (many body)  
 Valentin Kasper (many body, ML)  
 Reiko Yamada (quantum music)

**Ex-members and collaborators:** Aditi Sen De, Ujjwal Sed (HRI, Alahabad), Manab Bera (IIT), Fran ois Dubin (CNRS), G. John Lapeyre (CSIC), Luca Tagliacozzo (UB), Alessio Celi (IQOQI/UAB), Matthieu Alloing (Paris), Tomek Sowiński (IFPAN), Phillip Hauke (Trento), Omjyoti Dutta (GMV), Christian Trefzger (EC), Kuba Zakrzewski (UJ, Cracow), Mariusz Gajda (IFPAN), Boris Malomed (Haifa), Ulrich Ebling (Kyoto), Bruno Julia D az (UB), Christine Muschik (UoT), Marek Ku , Remigiusz Augusiak (CFT), Julia Stasińska (IFPAN), Alexander Streltsov (FUB), Ravindra Chhajlany (UAM), Fernando Cucchietti (MareNostrum), Anna Sanpera (UAB), Veronica Ahufinger (UAB), Tobias Grass (JQI,UMD/NIST), Jordi Tura (MPQ), Alexis Chac n (Los Alamos), Arnau Riera (BCN), Przemek Grzybowski (UAM), Swapan Rana (UW, Warsaw), Shi-Ju Ran (CNU), Ir n e Fr rot (ICFO-QIT), Giulia de Rosi (UPC), Maria Maffei (Grenoble), Christos Charampoulos (IFICS), Angelo Piga (WWW Institute), Zahra Khanian (TUM), Emilio Pisanty (MBI Berlin), Marcelo Ciappina (China-Technion), Emanuele Tirrito (SISSA), Luca Barbiero (Politecnica Torino), Debraj Rakshit (ISS India)



# Outline: Cold atoms meet lattice gauge theory

## 1. Quantum simulators (and annealers)

- 1.1 Ideology
- 1.2 Paradigmatic examples
- 1.3 Royal Society initiative

## 2. Cold atoms meet lattice gauge theory

- 2.1 Schwinger model and bosonic Schwinger model
- 2.2 Strongly correlated bosons in a dynamical lattice
- 2.3 The synthetic Creutz-Hubbard model

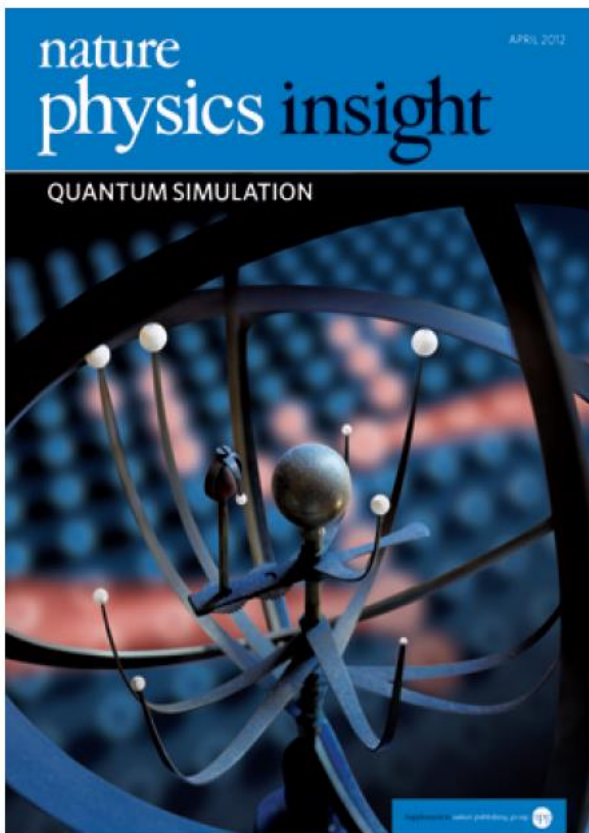
## 3. Experimental and experimentally friendly quantum simulators:

- a) Density dependent gauge fields
- b) Floquet engineering of  $Z_2$  gauge fields
- c) Local  $U(1)$  symmetry from spin-changing collisions
- d) Minimal  $SU(2)$  models for ultracold atom systems
- e) Non-Abelian gauge invariance from dynamical decoupling
- f) Rotor Jackiw-Rebbi model

## 4. Outlook: Conclusions and outlook



# 1. Quantum simulators (and annealers)



## COVER IMAGE

Before the advent of digital computers, sophisticated orreries were used to predict the positions and motions of astronomical bodies. Now quantum simulators hold the promise of providing insight into the behaviour and properties of complex quantum systems, in situations where classical computers reach their limits. Foreground image: © Michael Ventura/Alamy. Background image: © Immanuel Bloch/MPQ.

# Quantum Simulation

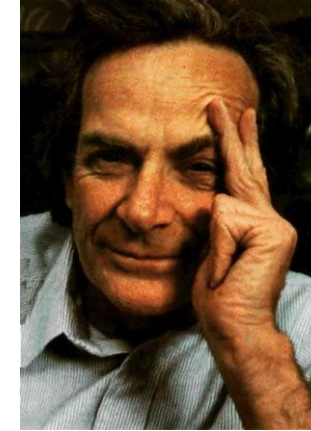
Jens Eisert<sup>6</sup>, Immanuel Bloch<sup>7</sup>, Maciej Lewenstein<sup>8</sup>, Stefan Kuhr<sup>9</sup>

## Introduction

The idea of quantum simulation goes back to Richard Feynman, who suggested that interacting quantum systems could be efficiently simulated employing other precisely controllable quantum systems, even in many instances in which such a simulation task is expected to be inefficient for standard classical computers [Feynman82]. In general, the classical simulation of quantum systems requires exponentially large resources, as the dimension of the underlying Hilbert space scales exponentially with the system size. This scaling may be significantly altered by employing appropriate representations of the quantum state valid in specific situations. Similarly, solutions of certain classical optimization problems, in particular NP-hard and NP-complete ones, require exponential resources. Numerical methods, such as tensor networks or the density-matrix renormalization group (DMRG) approach, as well as Quantum Monte Carlo sampling allow for computing of ground state properties in certain situations. Such classical simulation methods are generally applicable to restricted classes of problems and have their limitations. For example, the systems sizes that can be studied numerically on classical computers are often rather small and it seems unlikely that these classical tools will be powerful enough to provide a sufficient understanding of the full complexity of many-body quantum phenomena. In the language of complexity theory, approximating the ground-state energy of local Hamiltonian problems is QMA-hard, and time evolution under local Hamiltonians is BQP-complete, so both amount to computationally hard problems. Similarly, finding a ground-state energy of a classical spin glass, or solving the travelling salesman's problem, are computationally difficult. Quantum simulators promise to overcome some of these limitations.

## 1.1 Quantum Simulators: Ideology I

- There exist many interesting **quantum phenomena** (such as superconductivity).
- These phenomena may have important applications!
- These phenomena are often difficult to be described and understood with the help of standard computers.
- Maybe we can use another, simpler and better controllable quantum system to simulate, understand and control these phenomena (R.P. Feynman)? Such a system would thus work as quantum computer of special purpose, i.e.

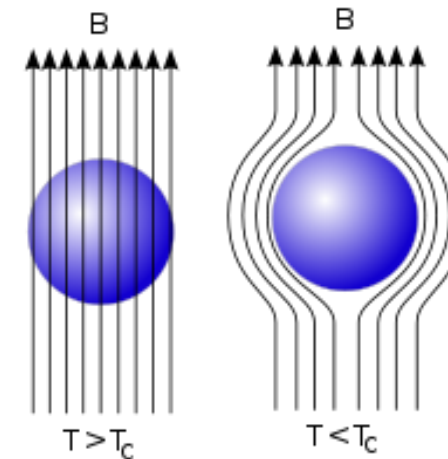


**QUANTUM SIMULATOR**



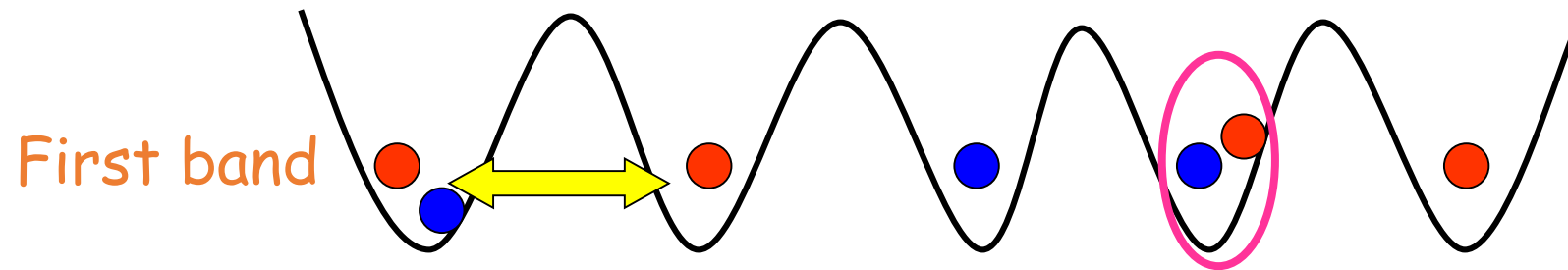
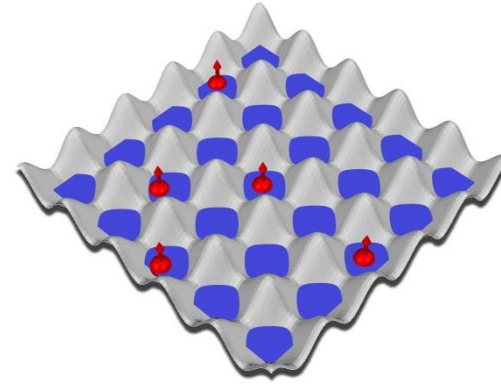
# Interesting quantum phenomenon: Superconductivity

- Superconductors are “ideal” conductors, they conduct electric currents without resistance.
- They conduct strong currents without losses.
- They can generate strong magnetic fields outside of them, but due to the Meissner-Ochsenfeld effect, they do not let magnetic fields enter them!
- Unfortunately, superconductors exist only at low temperatures: normally close to absolute zero,  $-270^{\circ}$  Celcius, “high temperature SC” at  $T > -166^{\circ}$  (boiling of liquid nitrogen).



- We (some of us) believe there exist a simple model that captures the phenomenon of high  $T_c$  superconductivity, the Hubbard model.
- Unfortunately, even this simple model is far too hard to simulate, and hard to understand with existing computers.
- So, why not trying to mimick it with atoms...

## Simple Hubbard model



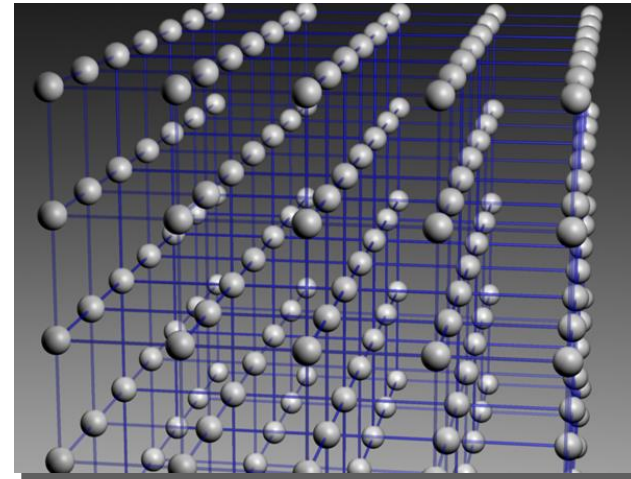
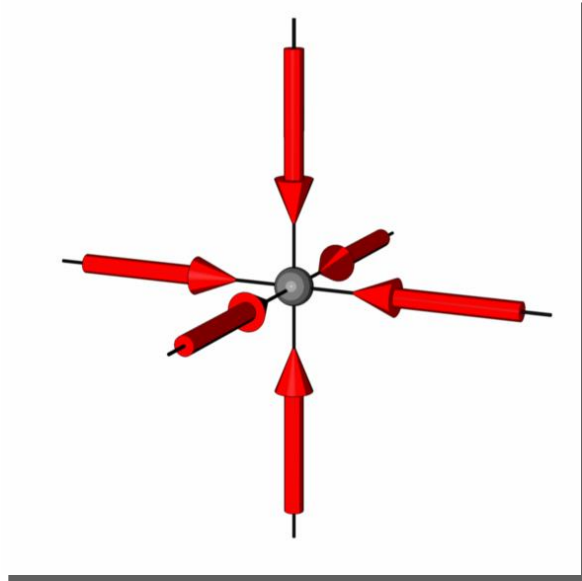
■ Tunneling

■ On site interactions

## (Fermi) Hubbard model

$$H = U \sum_i n_{i\downarrow} n_{i\uparrow} - \frac{1}{2} J \sum_{\langle ij \rangle, s} b_s^+ b_s + h.c. - \mu \sum_{i,s} n_{is}$$

# 3D Lattice Potential (by courtesy of M. Greiner, O. Mandel, T. Esslinger, I. Bloch, and T. Hänsch)



- Resulting potential consists of a simple cubic lattice
- BEC coherently populates more than **100,000** lattice sites

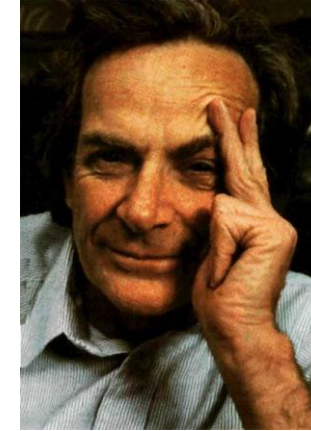
$V_0$  up to **22**  $E_{recoil}$

$\omega_r$  up to  $2\pi \cdot 30$  kHz

$n \approx$  **1-5** atoms on average per site

## 1.2 Quantum Simulators: Ideology II

- There exist many interesting **classical optimization problems** (such as spin glasses, travelling salesman...)
- These phenomena may have important applications!
- These phenomena are often difficult to be described and understood with the help of standard computers
- Maybe we can use another, simpler and better controllable quantum system to solve, understand and control these classical problems (D-Wave computers)? Such a system would thus work as quantum computer of special purpose, i.e.



**QUANTUM SIMULATOR/ANNEALER**

## What shall we simulate?

- Statics at zero temperature - ground state and its properties.
- Statics/equilibrium dynamics at non-zero temperature, or low energies.
- Dynamics (Hamiltonian, but out of equilibrium)
- Dissipative dynamics

## 1.2 Paradigmatic examples: Platforms/models

- Ultracold atoms in traps/on chips (QFT with  $\Psi^4$  interactions, or more...)
- Ultracold atoms in optical lattices (Hubbard models, spin models)
- Ultracold trapped ions (spin models with long range interactions)
- Rydberg atoms in optical tweezers
- Circuit QED
- Quantum dots arrays
- Josephson/superconducting qubits arrays (Ising spin glasses)
- Polariton condensates
- Photonic platforms (boson sampling)

# Hamiltonians

$$\text{Bosons: } \int dx \hat{\Psi}^\dagger(x) \left[ -\frac{\hbar^2 \nabla^2}{2m} + V(x) \right] \hat{\Psi}(x) \\ + \frac{4\pi\hbar^2 a}{m} \int dx \hat{\Psi}^\dagger(x) \hat{\Psi}^\dagger(x) \hat{\Psi}(x) \hat{\Psi}(x)$$

where  $[\hat{\Psi}(x), \hat{\Psi}(x')] = [\hat{\Psi}^\dagger(x), \hat{\Psi}^\dagger(x')] = 0$

$$[\hat{\Psi}(x), \hat{\Psi}^\dagger(x')] = \delta(x-x')$$

+ Many components



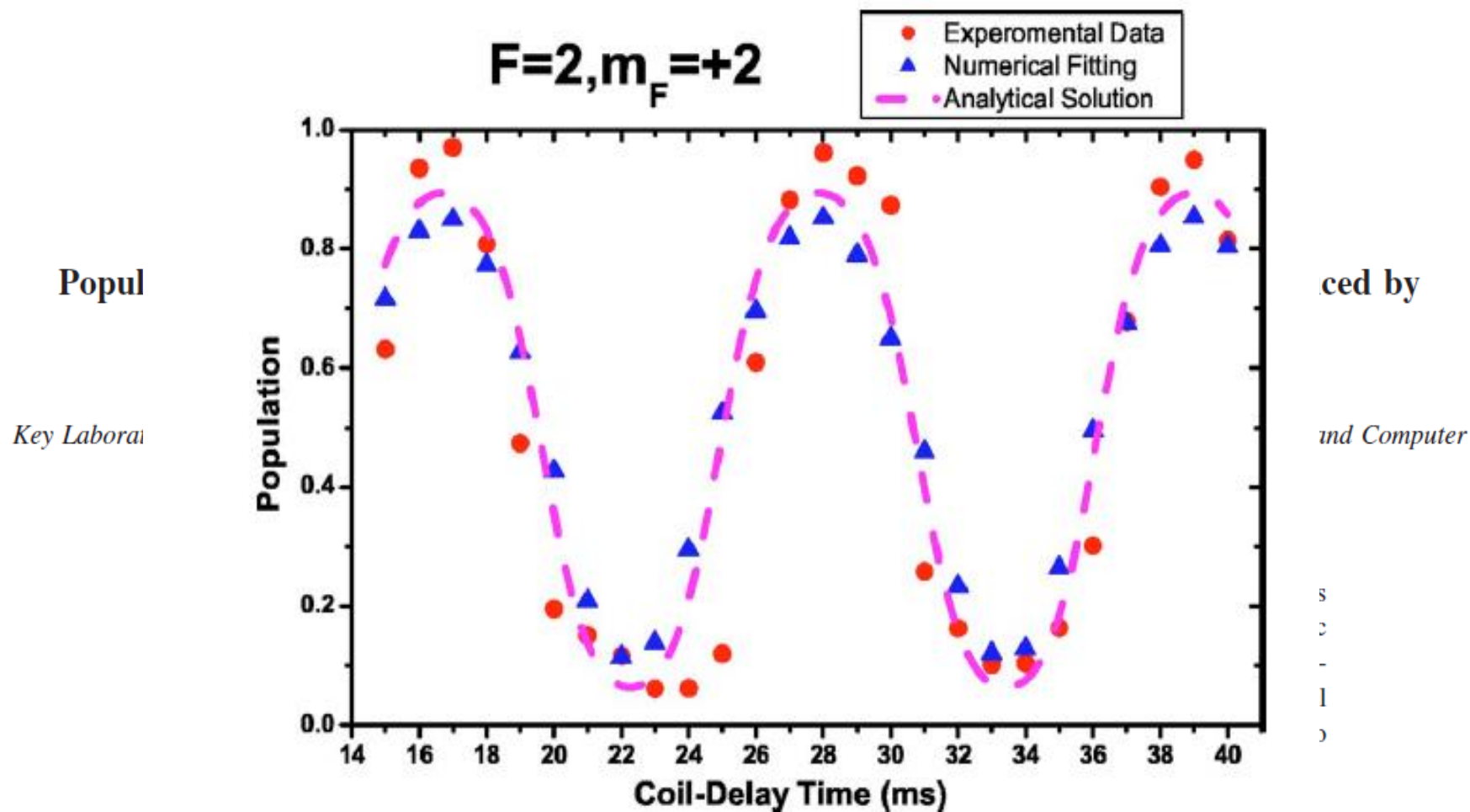


FIG. 5. (Color online) The experimental data and analyzing results: The population oscillation of  $|F=2, m_F=+2\rangle$  state versus coil delay time. The red (circles) represent the experimental data, while the blue (triangles) represent the numerical fitting. The dashed line is drawn by the analytic solution from above theoretical deducing.

Hamiltonians:

Fermions:

$$\sum_{\sigma=\uparrow,\downarrow} \int dx \hat{\Psi}_{\sigma}^{\dagger}(x) \left[ -\frac{\hbar^2 \nabla^2}{2m} + V(x) \right] \hat{\Psi}_{\sigma}(x)$$
$$+ \frac{2\pi\hbar a}{m} \int dx \hat{\Psi}_{\uparrow}^{\dagger}(x) \hat{\Psi}_{\downarrow}^{\dagger}(x) \hat{\Psi}_{\downarrow}(x) \hat{\Psi}_{\uparrow}(x)$$

where

$$\{ \hat{\Psi}_{\sigma}(x), \hat{\Psi}_{\sigma'}^{\dagger}(x') \} = \delta(x-x') \delta_{\sigma\sigma'}$$

$$\{ \hat{\Psi}_{\sigma}(x), \hat{\Psi}_{\sigma'}(x') \} = \{ \hat{\Psi}_{\sigma}^{\dagger}(x), \hat{\Psi}_{\sigma'}^{\dagger}(x') \} = 0$$

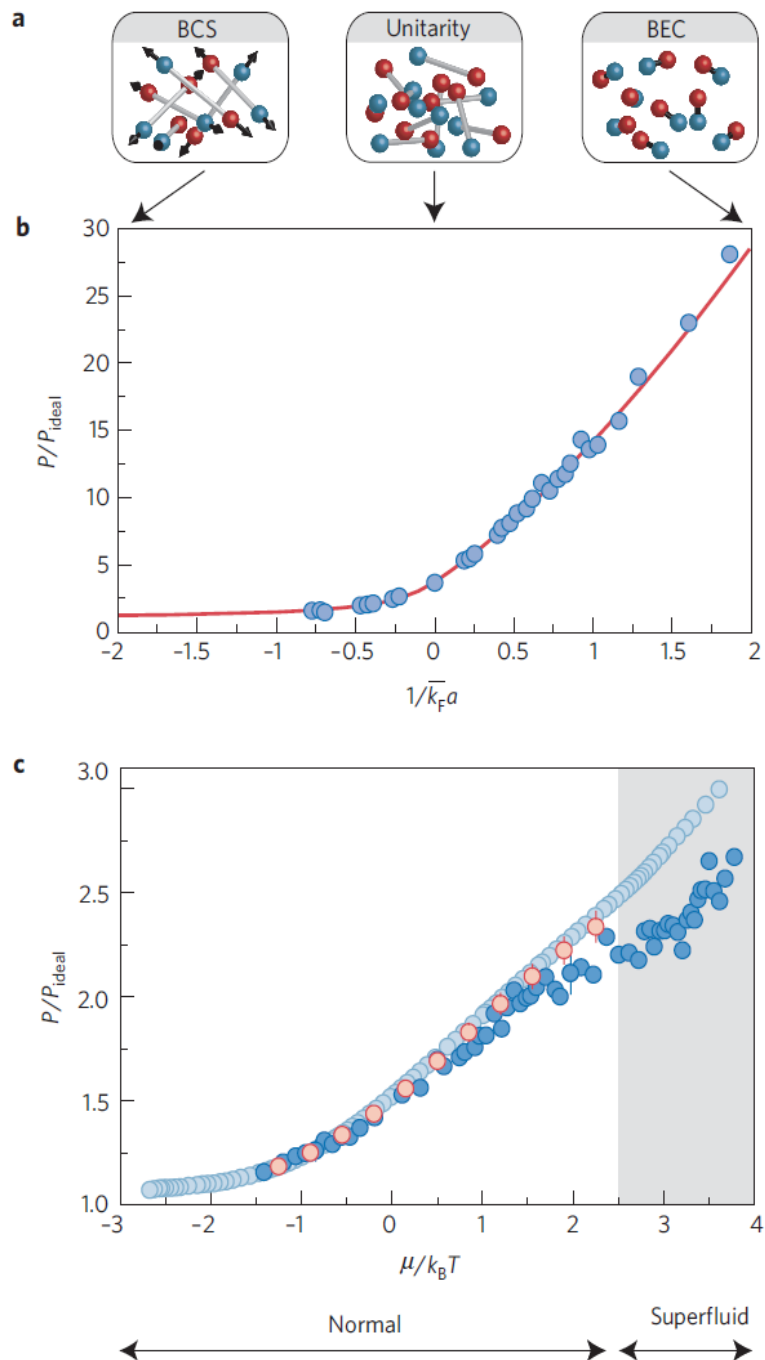


**Figure 1 | Equations of state of interacting ultracold Fermi gases.**

**a**, Schematic representation of the BEC-BCS crossover. For weak attractive interactions, atoms of opposite spin and momentum form Cooper pairs whose spatial extent greatly exceeds the mean interparticle distance. In the opposite limit of strongly attractive interactions, the gas is made of tightly bound molecules forming a BEC. In the middle of the crossover between the BCS and BEC regimes, the scattering length diverges at the unitary limit, leading to a strongly correlated state of matter. **b**, Equation of state of the ground state of a Fermi gas in the BEC-BCS crossover, expressed as the pressure normalized by the non-interacting pressure as a function of the interaction parameter  $1/\overline{k_F}a$ . (For the definition of the Fermi momentum  $\overline{k_F}$ , see ref. 18.) The solid red line is obtained from the fixed-node diffusion Monte Carlo simulation of ref. 140 and the blue dots are experimental data from ref. 18. Panel reproduced with permission from ref. 18, © 2010 AAAS.

**c**, Finite-temperature equation of state of the unitary Fermi gas. The dark (light) blue dots are the experimental data from ref. 40 (ref. 19) and the red dots are the bold diagrammatic Monte Carlo data from ref. 41. The grey area indicates the superfluid phase; the location of the normal/superfluid phase transition is taken from ref. 19. Panel reproduced with permission from ref. 19, © 2012 AAAS.

**Navon, N., Nascimbène, S., Chevy, F. & Salomon, C. The equation of state of a low-temperature Fermi gas with tunable interactions. *Science* 328, 729732 (2010).**

**Ku, M. J. H., Sommer, A. T., Cheuk, L. W. & Zwierlein, M. W. Revealing the superfluid Lambda transition in the universal thermodynamics of a unitary Fermi gas. *Science* 335, 563567 (2012).**

## 1.2 Paradigmatic examples: Platforms/models

- Ultracold atoms in traps/on chips (QFT with  $\Psi^4$  interactions, or more...)
- Ultracold atoms in optical lattices (Hubbard models, spin models)
- Ultracold trapped ions (spin models with long range interactions)
- Rydberg atoms in optical tweezers
- Circuit QED
- Quantum dots arrays
- Josephson/superconducting qubits arrays (Ising spin glasses)
- Polariton condensates
- Photonic platforms (boson sampling)

# Hamiltonians (Bose-Hubbard model)

Bosons:

$$-t \sum_{\langle i, j \rangle} (b_i^\dagger b_j + b_j^\dagger b_i) + \frac{U}{2} \sum_i n_i (n_i - 1) - \mu \sum_i n_i$$

$n_i = b_i^\dagger b_i$

$$[b_i, b_j] = [b_i^\dagger, b_j^\dagger] = 0 \quad [b_i, b_j^\dagger] = \delta_{ij}$$

# Phase diagram of the Bose-Hubbard model

62 Bose-Hubbard models: methods of treatment

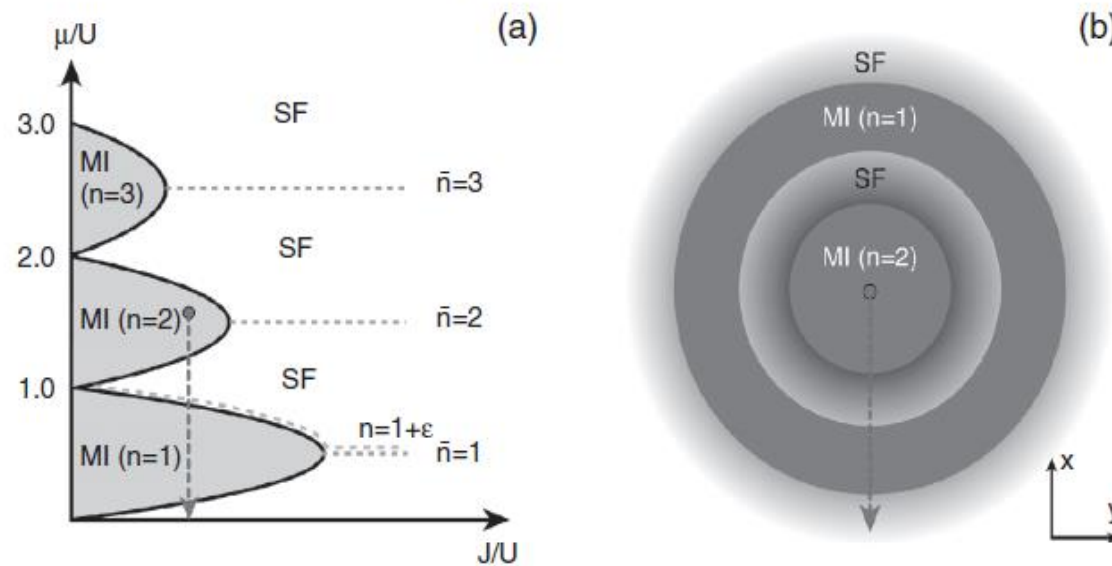


**Figure 5.1** (a) Schematic zero-temperature phase diagram of the Bose-Hubbard model displaying the celebrated Mott-insulator (MI) lobes for  $n = \bar{n}_0 = 1, 2, 3$ . The dashed line corresponds to integer superfluid density  $\langle \hat{n} \rangle = 1, 2, 3$ . Such a diagram can be obtained using the perturbative mean-field approach of Section 5.4. In the figure  $J$  denotes tunneling term ( $t$ ) in eqn (5.1). (b) MI and superfluid regions in an harmonic trap with MI for  $\bar{n} = 2$  in the center. The so-called ‘wedding cake’ structure extends from the center to the edge of the cloud, where the chemical potential vanishes. From Bloch *et al.* (2008). Figure in color online.

# In si don

Nathan

The obser  
of ultraco  
experime  
example c  
temperatu  
spatially  
quantum  
pretation  
resolved,  
gas as it c  
ing direc  
superfluid  
pressibilit  
insulator  
Mott insu  
orem. Fu  
perature  
complete  
lated Bos  
fluctuatio

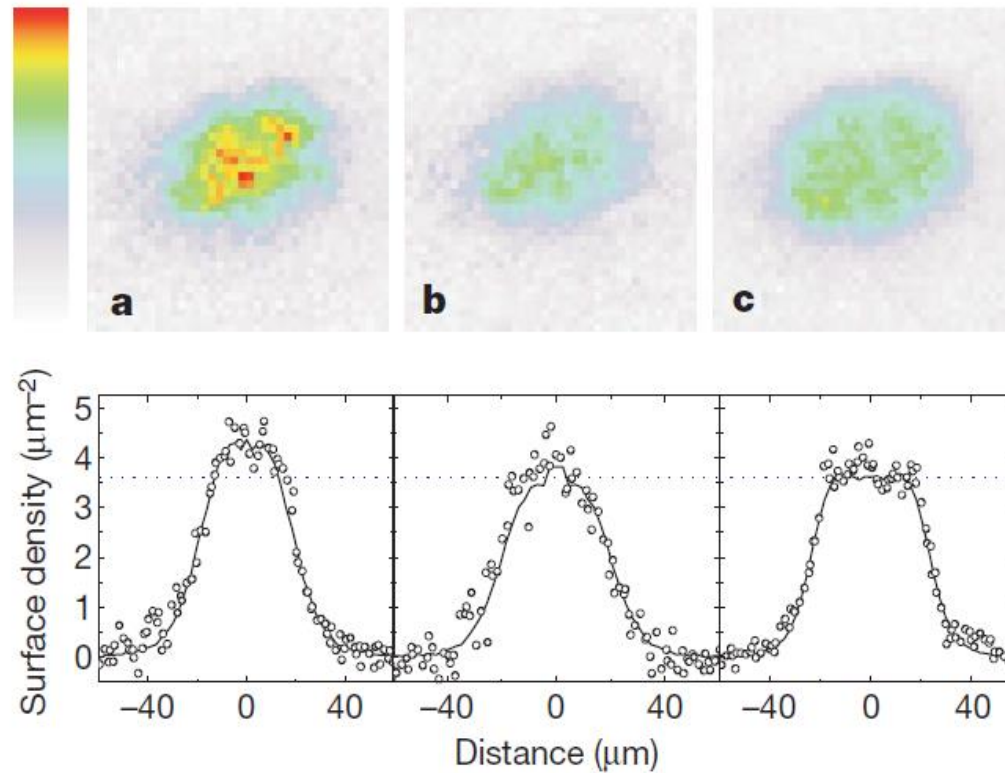


**Figure 1 | False-colour absorption images and line cuts along major axis of density profiles for  $N = 7,500$  ultracold caesium atoms at scattering length  $a = 310a_B$  in 2D optical lattices. **a**, Superfluid regime (shallow lattice  $V = 2.4E_R$ ); **b**, phase transition regime (medium lattice depth  $V = 9.4E_R$ ); and **c**, Mott-insulator regime (deep lattice  $V = 22E_R$ ). Images are averaged over three experiment repetitions. The colour scale shows linear variation with density from zero to the peak value of  $5.4 \mu\text{m}^{-2}$ . Line cuts are taken along the major axis, and compared to radial average of density (solid line) over the entire image as described in text. The blue horizontal dotted line indicates the density of one atom per site.**

# ERS lating

the horizontal  
ing  $d = \lambda/2 =$   
 $\sqrt{\omega_x^2 x^2 + \omega_y^2 y^2}/2$   
l the geometric  
 $v_r = \sqrt{\omega_x \omega_y} =$   
ction (a weak  
hods). Vertical  
ical lattice with  
ing at an angle  
ket of width  
d into a single  
cal tunnelling.  
by varying the  
atomic sample  
ref. 13.

ption imaging,  
the horizontal  
ation such that  
on the object  
atmosphere

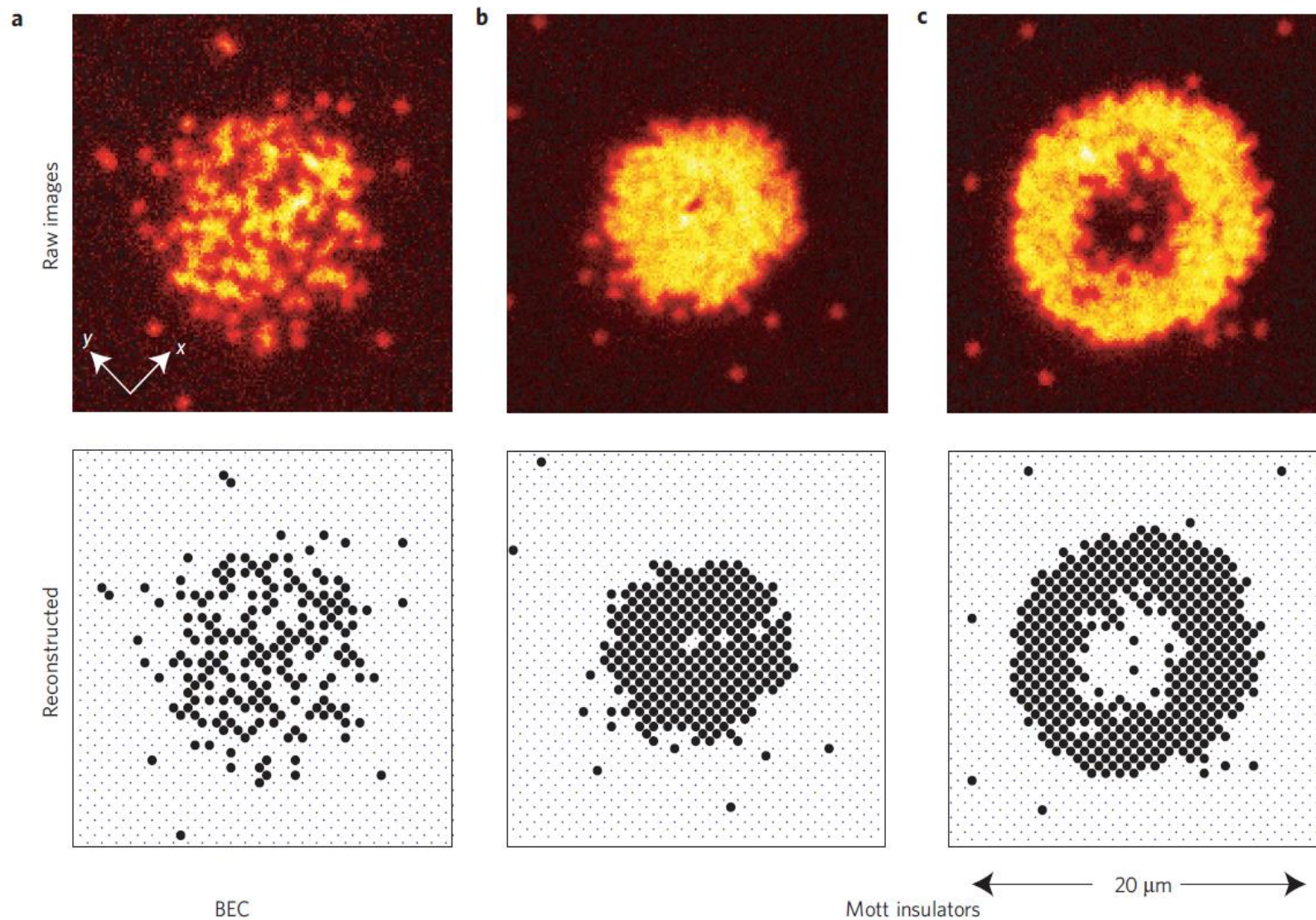


**Figure 2 | Single-atom resolved images of a BEC and Mott insulators. a,** A weakly interacting BEC. **b,c,** Strongly interacting Mott insulators in the atomic limit. The top row shows the raw-data fluorescence images. For higher atom numbers (**c**) a shell structure develops with a doubly occupied core in the centre. Owing to light-induced losses, the parity of the occupation number is detected in experiments (Box 2). The bottom row shows the results of an image-analysis algorithm through which the particle positions were reconstructed. Figure reproduced from ref. 80.



# Hamiltonians (Fermi - Hubbard)

Fermions

$$-t \sum_{\sigma} \sum_{\langle i,j \rangle} (f_{i\sigma}^{\dagger} f_{j\sigma} + f_{j\sigma}^{\dagger} f_{i\sigma}) + U \sum_i n_{i\uparrow} n_{i\downarrow} - \sum_{\sigma} \mu_{\sigma} \sum_i n_{i\sigma}$$

$$n_{i\sigma} = f_{i\sigma}^{\dagger} f_{i\sigma}$$

$$\{f_{i\sigma}, f_{i'\sigma'}^{\dagger}\} = \{f_{i\sigma}^{\dagger}, f_{i'\sigma'}\} = 0$$

$$\{f_{i\sigma}, f_{j\sigma'}\} = \delta_{ij} \delta_{\sigma\sigma'}$$

## LETTER

doi:10.1038/nature22362

### A cold-atom Fermi-Hubbard antiferromagnet

Anton Mazurenko<sup>1</sup>, Christie S. Chiu<sup>1</sup>, Geoffrey Ji<sup>1</sup>, Maxwell F. Parsons<sup>1</sup>, Márton Kanász-Nagy<sup>1</sup>, Richard Schmidt<sup>1</sup>, Fabian Grusdt<sup>1</sup>, Eugene Demler<sup>1</sup>, Daniel Greif<sup>1</sup> & Markus Greiner<sup>1</sup>

Exotic phenomena in systems with strongly correlated electrons emerge from the interplay between spin and motional degrees of freedom. For example, doping an antiferromagnet is expected to give rise to pseudogap states and high-temperature superconductors<sup>1</sup>. Quantum simulation<sup>2-8</sup> using ultracold fermions in optical lattices could help to answer open questions about the doped Hubbard Hamiltonian<sup>9-14</sup>, and has recently been advanced by quantum gas microscopy<sup>15-20</sup>. Here we report the realization of an antiferromagnet in a repulsively interacting Fermi gas on a two-dimensional square lattice of about 80 sites at a temperature of 0.25 times the tunnelling energy. The antiferromagnetic long-range order manifests through the divergence of the correlation length, which reaches the size of the system, the development of a peak in the spin structure factor and a staggered magnetization that is close to the ground-state value. We hole-dope the system away from half-filling, towards a regime in which complex many-body states are expected, and find that strong magnetic correlations persist at the antiferromagnetic ordering vector up to dopings of about 15 per cent. In this regime, numerical simulations are challenging<sup>21</sup> and so experiments provide a valuable benchmark. Our results demonstrate that microscopy of cold atoms in optical lattices can help us to understand the low-temperature Fermi-Hubbard model.

# Simulating interesting systems - High $T_c$ - superconductivity

LETTER RESEARCH

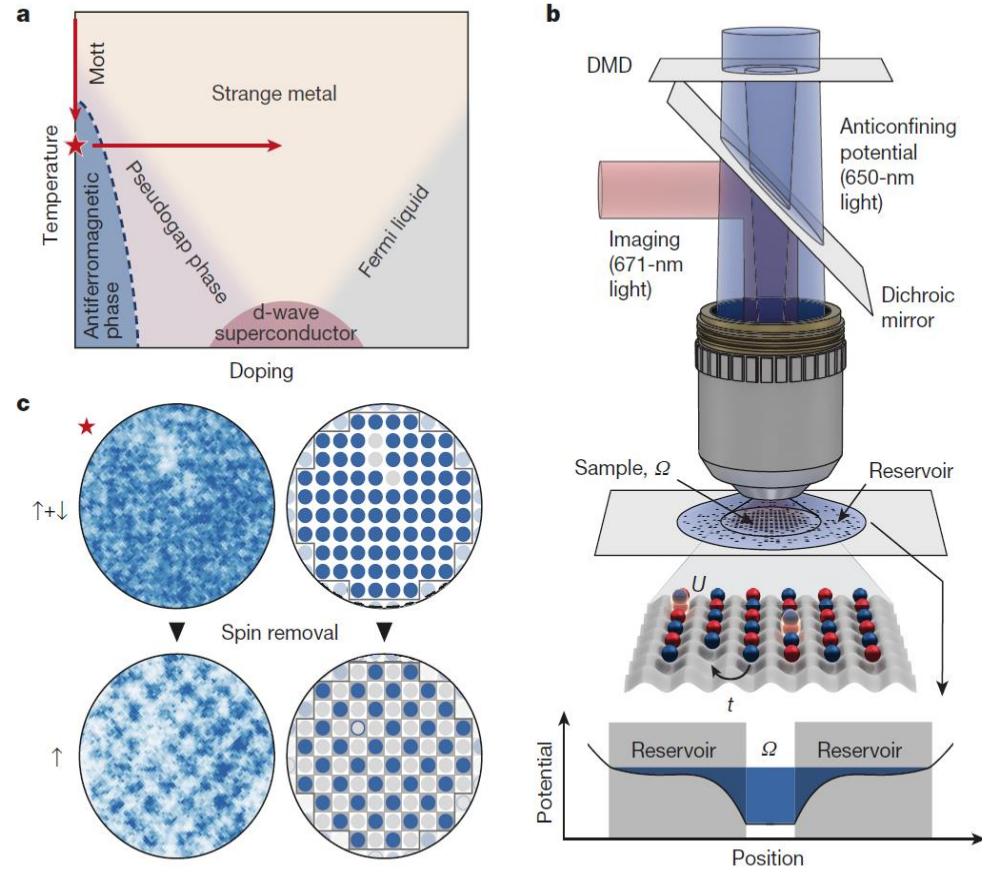


**Figure 1 | Probing antiferromagnetism in the Hubbard model with a quantum gas microscope.** **a**, Schematic of the two-dimensional Hubbard phase diagram, including predicted phases. We explore the trajectories traced by the red arrows for a Hubbard model with  $U/t = 7.2(2)$ . The strongest antiferromagnetic order is observed at the starred point. **b**, Experimental set-up. We trap  $^6\text{Li}$  atoms in a two-dimensional square optical lattice. We use the combined potential of the optical lattice and the anticonfinement that is generated by the digital micromirror device (DMD) to trap the atoms in a central sample  $\Omega$  of homogeneous density,

surrounded by a dilute reservoir, as shown in the plot. The system is imaged with 671-nm light along the same beam path as the projected 650-nm potential, and separated from it by a dichroic mirror. **c**, Exemplary raw (left) and processed (right) images of the atomic distribution of single experimental realizations, with both spin components present (upper; corresponding to the starred point in **a**) and with one spin component removed (lower). The observed checkerboard pattern in the spin-removed images indicates the presence of an antiferromagnet.

# Simulating interesting systems - High $T_c$ - superconductivity

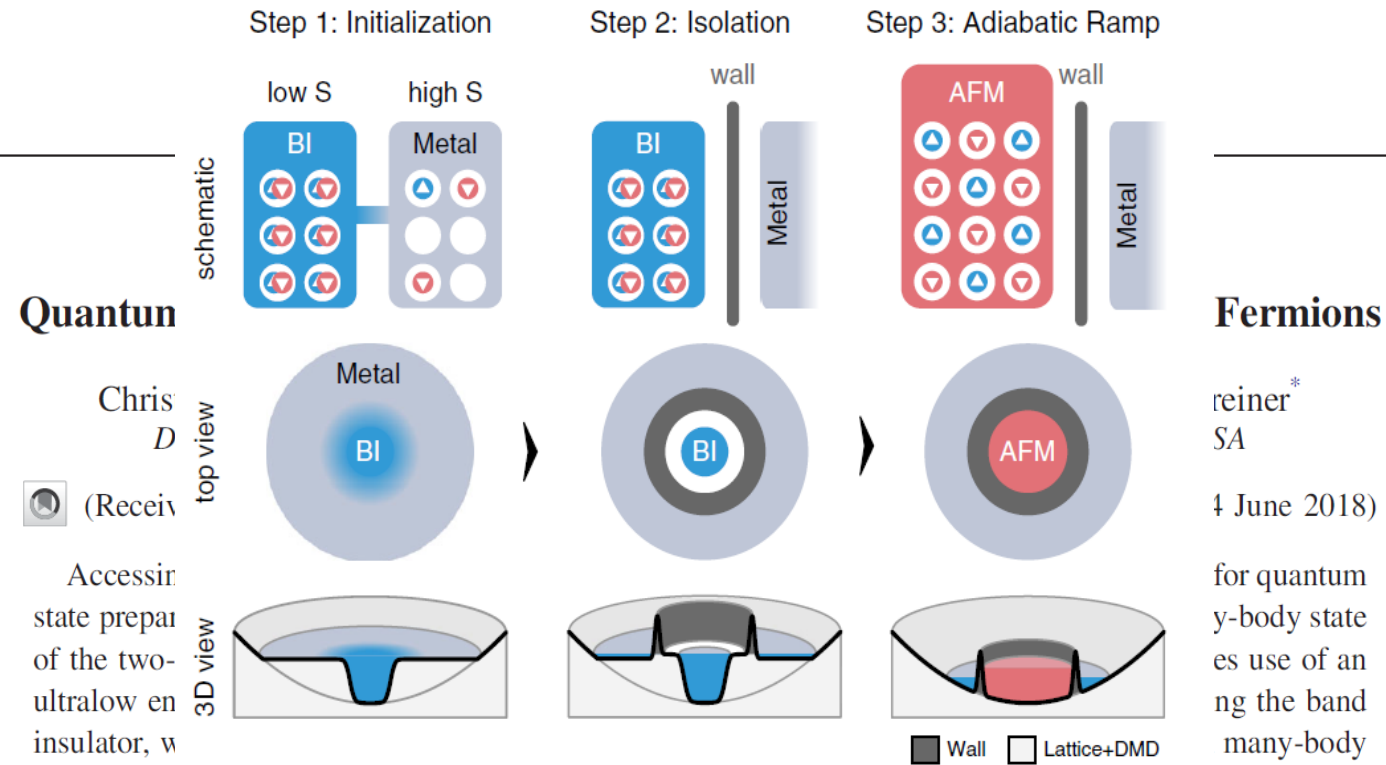


FIG. 1. Illustration of the quantum state engineering scheme. (Top row) A low-density metallic state removes entropy from a band insulator (BI), after which the two states can be isolated thermally. The BI can then be ramped into an antiferromagnetic (AFM) state by increasing the number of available sites. (Middle row) Map of density inhomogeneity and states in our experimental setup. (Bottom row) We implement our scheme by engineering optical potential landscapes to change the Hamiltonian at each step (see main text and [32]).

<sup>9</sup>Johannes Gutenberg-Universität, Institut für Physik, 55128 Mainz, Germany

<sup>10</sup>Institute of Theoretical Physics and Astronomy, Vilnius University, LT-10257 Vilnius, Lithuania

<sup>11</sup>Department of Physics, Capital Normal University, 100048 Beijing, China

<sup>12</sup>Forschungszentrum Jülich, Institute of Quantum Control, Peter Grünberg Institut (PGI-8), 52425 Jülich, Germany

<sup>13</sup>Institute for Theoretical Physics, University of Cologne, 50937 Köln, Germany

<sup>14</sup>Instituto de Física Teórica, UAM/CSIC, Universidad Autónoma de Madrid, Madrid, Spain

<sup>15</sup>Departament de Física Quàntica i Astrofísica and Institut de Ciències del Cosmos (ICCUB), Universitat de Barcelona, 08028 Barcelona, Catalonia, Spain

<sup>16</sup>International School for Advanced Studies (SISSA), 34136 Trieste, Italy

<sup>17</sup>Center for Quantum Physics, University of Innsbruck, 6020 Innsbruck, Austria

<sup>18</sup>Institute for Quantum Optics and Quantum Information of the Austrian Academy of Sciences, 6020 Innsbruck, Austria

<sup>19</sup>Racah Institute of Physics, The Hebrew University of Jerusalem, Jerusalem 91904, Israel

<sup>20</sup>ICREA, Passeig Lluís Companys 23, 08010 Barcelona, Spain

The central idea of this review is to consider quantum field theory models relevant for particle physics and replace the fermionic matter in these models by a bosonic one. This is mostly motivated by the fact that bosons are more “accessible” and easier to manipulate for experimentalists, but this “substitution” also leads to new physics and novel phenomena. It allows us to gain new information about among other things confinement and the dynamics of the deconfinement transition. We will thus consider bosons in dynamical lattices corresponding to the bosonic Schwinger or  $Z_2$  Bose-Hubbard models. Another central idea of this review concerns atomic simulators of paradigmatic models of particle physics theory such as the Creutz-Hubbard ladder, or Gross-Neveu-Wilson and Wilson-Hubbard models. Finally, we will briefly describe our efforts to design experimentally friendly simulators of these and other models relevant for particle physics.

## 2. Cold atoms meet lattice gauge theories and more...

# 2.1 Schwinger model

## LETTER

doi:10.1038/nature18318

### Real-time dynamics of lattice gauge theories with a few-qubit quantum computer

Esteban A. Martinez<sup>1\*</sup>, Christine A. Muschik<sup>2,3\*</sup>, Philipp Schindler<sup>1</sup>, Daniel Nigg<sup>1</sup>, Alexander Erhard<sup>1</sup>, Markus Heyl<sup>2,4</sup>, Philipp Hauke<sup>2,3</sup>, Marcello Dalmonte<sup>2,3</sup>, Thomas Monz<sup>1</sup>, Peter Zoller<sup>2,3</sup> & Rainer Blatt<sup>1,2</sup>

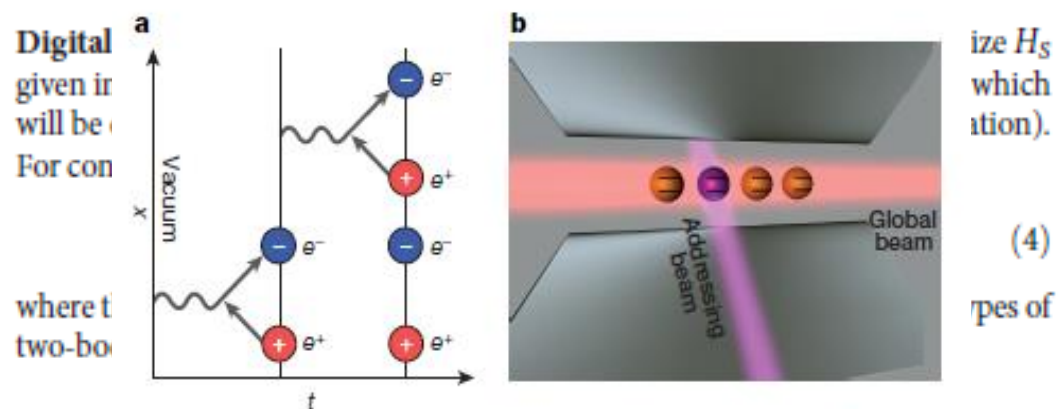


**Figure 1 | Quantum simulation of the Schwinger mechanism.** **a**, The instability of the vacuum due to quantum fluctuations is one of the most fundamental effects in gauge theories. We simulate the coherent real-time dynamics of particle–antiparticle creation by realizing the Schwinger model (one-dimensional quantum electrodynamics) on a lattice, as described in the main text. **b**, The experimental setup for the simulation consists of a linear Paul trap, where a string of  $^{40}\text{Ca}^+$  ions is confined. The electronic states of each ion, depicted as horizontal lines, encode a spin  $|\uparrow\rangle$  or  $|\downarrow\rangle$ . These states can be manipulated using laser beams (see Methods for details).

Gauge theories are fundamental to our understanding of interactions between the elementary constituents of matter as mediated by gauge bosons<sup>1,2</sup>. However, computing the real-time dynamics in gauge theories is a notorious challenge for classical computational methods. This has recently stimulated theoretical effort, using Feynman’s idea of a quantum simulator<sup>3,4</sup>, to devise schemes for simulating such theories on engineered quantum-mechanical devices, with the difficulty that gauge invariance and the associated local conservation laws (Gauss laws) need to be implemented<sup>5–7</sup>. Here we report the experimental demonstration of a digital quantum simulation of a lattice gauge theory, by realizing (1 + 1)-dimensional quantum electrodynamics (the Schwinger model<sup>8,9</sup>) on a few-qubit trapped-ion quantum computer. We are interested in the real-time evolution of the Schwinger mechanism<sup>10,11</sup>, describing the instability of the bare vacuum due to quantum fluctuations, which manifests itself in the spontaneous creation of electron–positron pairs. To make efficient use of our quantum resources, we map the original problem to a spin model by eliminating the gauge fields<sup>12</sup> in favour of exotic long-range interactions, which can be directly and efficiently implemented on an ion trap architecture<sup>13</sup>. We explore the Schwinger mechanism of particle–antiparticle generation by monitoring the mass production and the vacuum persistence amplitude. Moreover, we track the real-time evolution of entanglement in the system, which illustrates how particle creation and entanglement generation are directly related. Our work represents a first step towards quantum simulation of high-energy theories using atomic physics experiments—the long-term intention is to extend this approach to real-time quantum simulations of non-Abelian lattice gauge theories.

# 2.1 Bosonic Schwinger model

## Confinement and Lack of Thermalization after Quenches in the Bosonic Schwinger Model

Titas Chanda<sup>1,\*</sup>, Jakub Zakrzewski<sup>1,2</sup>, Maciej Lewenstein<sup>3,4</sup> and Luca Tagliacozzo<sup>5,6</sup>

<sup>1</sup>*Instytut Fizyki Teoretycznej, Uniwersytet Jagielloński, Łojasiewicza 11, 30-348 Kraków, Poland*

<sup>2</sup>*Mark Kac Complex Systems Research Center, Jagiellonian University in Krakow, Łojasiewicza 11, 30-348 Kraków, Poland*

<sup>3</sup>*ICFO-Institut de Ciències Fotòniques, The Barcelona Institute of Science and Technology, Av. Carl Friedrich Gauss 3, 08860 Castelldefels (Barcelona), Spain*

<sup>4</sup>*ICREA, Passeig Lluís Companys 23, 08010 Barcelona, Spain*

<sup>5</sup>*Department of Physics and SUPA, University of Strathclyde, Glasgow G4 0NG, United Kingdom*

<sup>6</sup>*Department de Física Quàntica i Astrofísica and Institut de Ciències del Cosmos (ICCUB), Universitat de Barcelona, Martí i Franquès 1, 08028 Barcelona, Catalonia, Spain*



(Received 7 October 2019; revised manuscript received 9 March 2020; accepted 31 March 2020; published 6 May 2020)

We excite the vacuum of a relativistic theory of bosons coupled to a  $U(1)$  gauge field in  $1+1$  dimensions (bosonic Schwinger model) out of equilibrium by creating a spatially separated particle-antiparticle pair connected by a string of electric field. During the evolution, we observe a strong confinement of bosons witnessed by the bending of their light cone, reminiscent of what has been observed for the Ising model [Nat. Phys. **13**, 246 (2017)]. As a consequence, for the timescales we are able to simulate, the system evades thermalization and generates exotic asymptotic states. These states are made of two disjoint regions, an external deconfined region that seems to thermalize, and an inner core that reveals an area-law saturation of the entanglement entropy.



## 2.1 Bosonic Schwinger model

*Model.*—The BSM Lagrangian density is given by  $\mathcal{L} = -[D_\mu\phi]^* D^\mu\phi - m^2|\phi|^2 - \frac{1}{4}F_{\mu\nu}F^{\mu\nu}$  [92], where  $\phi$  is the complex scalar field,  $D_\mu = (\partial_\mu + iqA_\mu)$  is the covariant derivative with  $q$  and  $A_\mu$  being the electronic charge and vector potential, respectively,  $m$  is the bare mass of the

## 2.1 Bosonic Schwinger model

$$\begin{aligned} \hat{H} = & \sum_j \hat{L}_j^2 + 2\{x[(m/q)^2 + 2x]\}^{1/2} \sum_j (\hat{a}_j^\dagger \hat{a}_j + \hat{b}_j \hat{b}_j^\dagger) \\ & - \frac{x^{3/2}}{[(m/q)^2 + 2x]^{1/2}} \sum_j [(\hat{a}_{j+1}^\dagger + \hat{b}_{j+1}) \hat{U}_j (\hat{a}_j + \hat{b}_j^\dagger) + \text{H.c.}], \end{aligned} \tag{1}$$

where  $\{\hat{a}_j^\dagger, \hat{a}_j\}$ ,  $\{\hat{b}_j^\dagger, \hat{b}_j\}$  are the bosonic creation-annihilation operators corresponding to charged particles and antiparticles, respectively,  $\hat{L}_j$  is the electric field

# 2.1 Bosonic Schwinger model

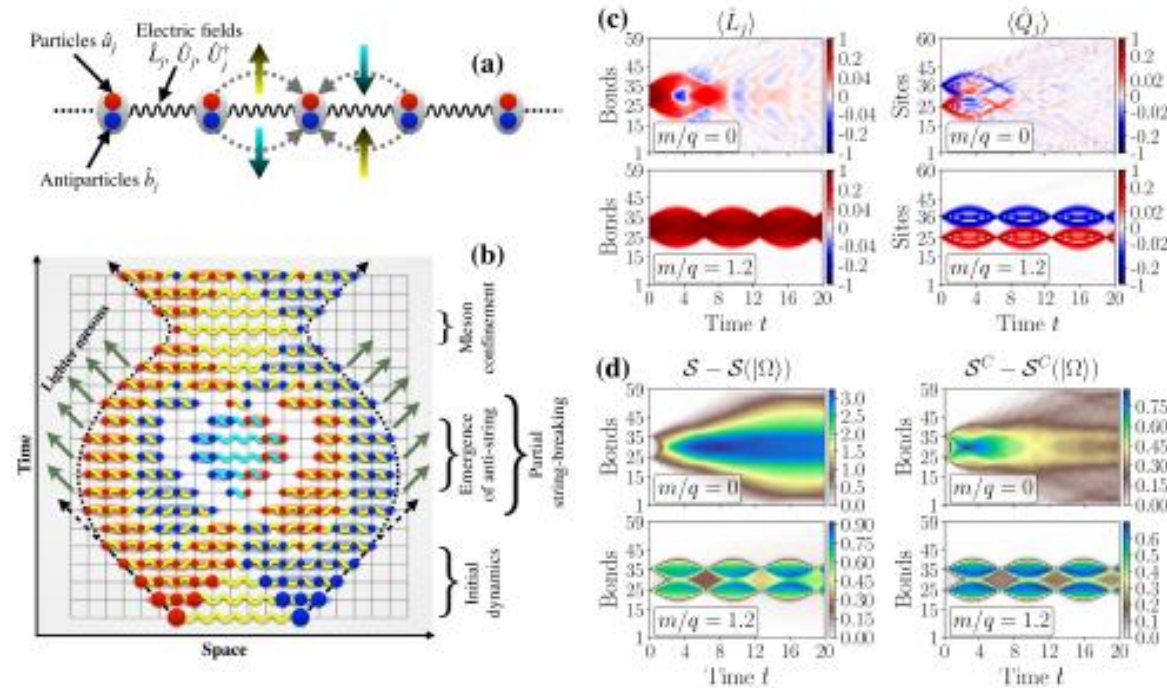


**Figure 1. The bosonic Schwinger model and its time-evolution [37]:** (a) Schematic depiction of BSM, where lattice sites are populated by particles (red circles) and antiparticles (blue circles) and the bonds between neighboring sites hold U(1) electric gauge fields. Left moving particles (antiparticles) raise (lower) the quantum state of the electric field in a corresponding bond, while the opposite holds for right moving bosons. (b) Sketch of the confining dynamics of BSM. The system is driven out of equilibrium by creating spatially separated particle-antiparticle pair connected by a string of electric field (a yellow wiggly line). The strong confinement of bosons bends the trajectory of both excitations. New dynamical charges are created during the evolution that partially screen the electric field. However, the electric field oscillates coherently and may form an anti-string (cyan wiggly line), creating a central core of strongly correlated bosons that is very different from an equilibrium state. This strange central region survives despite the fact that the boson density in the central region may be depleted through the radiation of lighter mesons that can propagate freely. (c) Dynamics of the electric field  $\langle \hat{L}_j \rangle$  and the dynamical charge  $\langle \hat{Q}_j \rangle$ , and (d) the same for the total entanglement entropy  $\mathcal{S}$  measured across different bonds and its classical part  $\mathcal{S}^C$ .

# 2.2 Strongly correlated bosons in a dynamical lattice

PHYSICAL REVIEW LETTERS **121**, 090402 (2018)

---

## Strongly Correlated Bosons on a Dynamical Lattice

Daniel González-Cuadra,<sup>1</sup> Przemysław R. Grzybowski,<sup>1,2</sup> Alexandre Dauphin,<sup>1</sup> and Maciej Lewenstein<sup>1,3</sup>

<sup>1</sup>*ICFO-Institut de Ciències Fotòniques, The Barcelona Institute of Science and Technology,  
Av. Carl Friedrich Gauss 3, 08860 Barcelona, Spain*

<sup>2</sup>*Faculty of Physics, Adam Mickiewicz University, Umultowska 85, 61-614 Poznań, Poland*

<sup>3</sup>*ICREA, Passeig Lluís Companys 23, 08010 Barcelona, Spain*



(Received 23 February 2018; published 30 August 2018)

We study a one-dimensional system of strongly correlated bosons on a dynamical lattice. To this end, we extend the standard Bose-Hubbard Hamiltonian to include extra degrees of freedom on the bonds of the lattice. We show that this minimal model exhibits phenomena reminiscent of fermion-phonon models. In particular, we discover a bosonic analog of the Peierls transition, where the translational symmetry of the underlying lattice is spontaneously broken. This provides a dynamical mechanism to obtain a topological insulator in the presence of interactions, analogous to the Su-Schrieffer-Heeger model for electrons. We characterize the phase diagram numerically, showing different types of bond order waves and topological solitons. Finally, we study the possibility of implementing the model using atomic systems.

DOI: [10.1103/PhysRevLett.121.090402](https://doi.org/10.1103/PhysRevLett.121.090402)

## 2.2 Strongly correlated bosons in a dynamical lattice

In this section, we will explore a further simplification that also leads to interesting phenomena in related models. We start from the simplest LGT with dynamical matter, ie. a one-dimensional chain of bosons coupled to a  $\mathbb{Z}_2$  gauge field [43],

$$H_{\mathbb{Z}_2} = -\alpha \sum_i \left( b_i^\dagger \sigma_{i,i+1}^z b_{i+1} + \text{H.c.} \right) + \beta \sum_i \sigma_{i,i+1}^x, \quad (3.1)$$

Although a quantum simulation of the full 1D chain is still lacking, the minimal building block of this model, a gauge-invariant correlated tunnelling term, has already been implemented with ultracold atoms using Floquet engineering [25]. We now consider adding extra terms to the Hamiltonian that break gauge invariance. In particular, we include the standard Bose-Hubbard Hamiltonian describing ultracold bosonic atoms in optical lattices [44],

$$H_{\text{BH}} = -t \sum_i \left( b_i^\dagger b_{i+1} + \text{H.c.} \right) + \frac{U}{2} \sum_i n_i (n_i - 1), \quad (3.2)$$

as well as a parallel field for the gauge degrees of freedom,  $H_\Delta = \frac{\Delta}{2} \sum_i \sigma_{i,i+1}^z$ . We denote the full Hamiltonian as the  $\mathbb{Z}_2$  Bose-Hubbard model ( $\mathbb{Z}_2$  BHM) [45];

$$H_{\mathbb{Z}_2\text{BH}} = H_{\mathbb{Z}_2} + H_{\text{BH}} + H_\Delta, \quad (3.3)$$

## 2.2 Strongly correlated bosons in a dynamical lattice

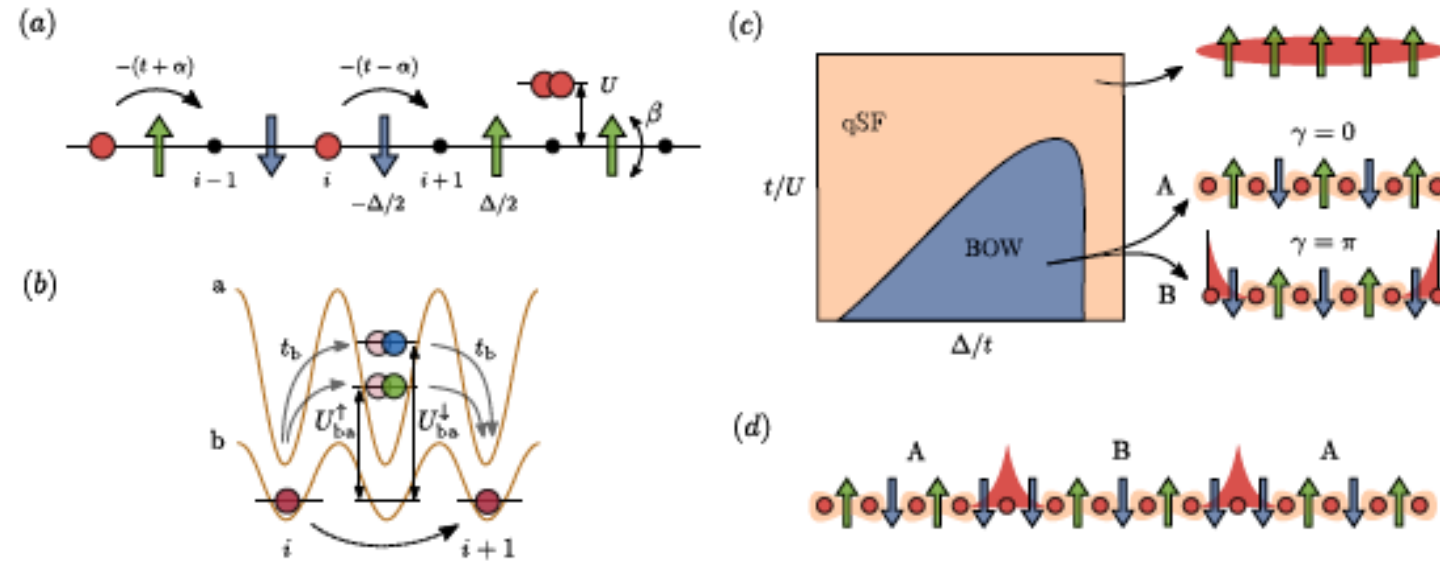


**Figure 2. Symmetry-breaking topological insulators [46]:** (a) Sketch of the  $\mathbb{Z}_2$  BHM (3.3). Bosonic particles (red spheres) hop on a one-dimensional lattice interacting among them and with  $\mathbb{Z}_2$  fields (arrows). The latter are located on lattice links and their configuration modifies the tunnelling strength. (b) The model describes a mixture of ultracold bosonic atoms in an optical lattice, where two hyperfine states of one deeply trapped species (green/blue spheres) simulates the  $\mathbb{Z}_2$  field [45]. The correlated tunnelling term can be obtained as a second-order density-dependent tunnelling process of the other species [47]. (c) Qualitative phase diagram at half filling. For strong enough Hubbard interactions, the system undergoes a bosonic Peierls transition from a qSF to a BOW phase where the field orders antiferromagnetically [48]. The two degenerate symmetry-broken patterns (A and B) give rise to insulating states, one of which manifests non-trivial topological properties such as localized edge states with a fractional bosonic number. (d) The presence of dynamical fields and the interplay between symmetry breaking and topological symmetry protection gives rise to strongly-correlated effects that are absent in a static lattice. In the figure, topological defects are shown between the different symmetry-broken field patterns, hosting fractional bosonic states that can move along the system's bulk [46,49].

## 2.2 Strongly correlated bosons in a dynamical lattice

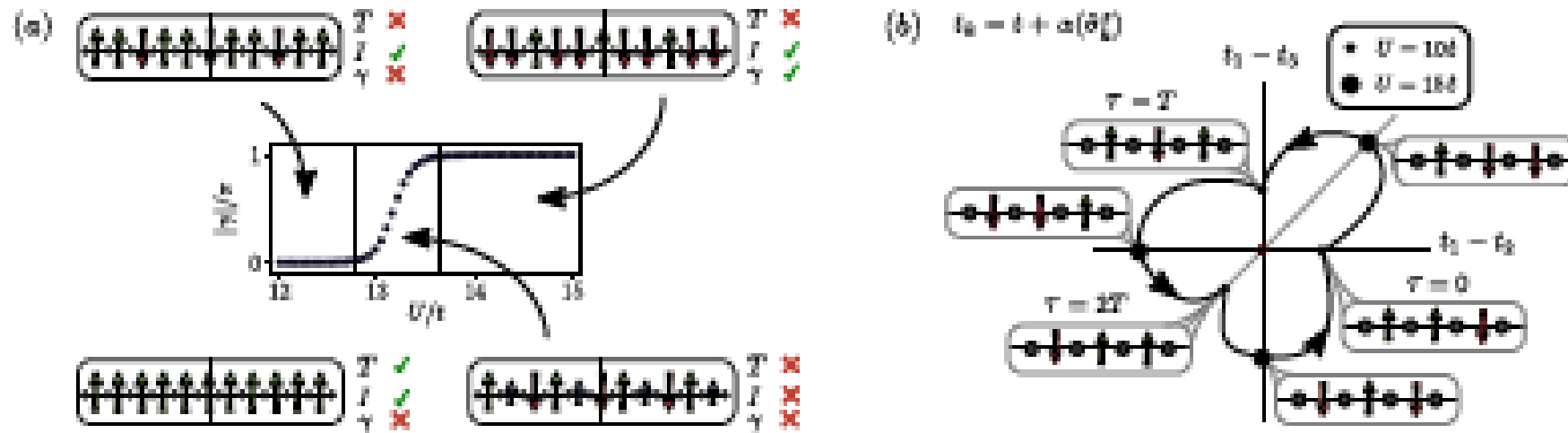


Figure 3. Emergent symmetry protection and fractional pumping [54]: (a) For fractional densities other than half filling, the SSB of translational invariance (T) can also break the protecting inversion symmetry (I). For  $\rho = 1/3$  and  $\rho = 2/3$ , the latter emerges again for sufficiently strong values of  $U$ , giving rise to non-trivial topology ( $\gamma = \pi$ ) while maintaining a trimmerized pattern along the phase transition [54]. (b) Such a symmetry-constrained transition can be employed to devise a self-adjusted pumping protocol, where the system travels adiabatically along the trivial and topological (three-fold) degenerate configurations. Each trivial-topological-trivial subcycle transport  $1/3$  of a boson [54]. In the figure,  $\langle \hat{\sigma}_k^z \rangle$ , with  $k = 1, 2, 3$  denotes the expectation value of the field within the repeating unit cell.

## 2.3 The synthetic Creutz-Hubbard model

PHYSICAL REVIEW X 7, 031057 (2017)

---

### Exploring Interacting Topological Insulators with Ultracold Atoms: The Synthetic Creutz-Hubbard Model

J. Jünemann,<sup>1,2</sup> A. Piga,<sup>3</sup> S.-J. Ran,<sup>3</sup> M. Lewenstein,<sup>3,4</sup> M. Rizzi,<sup>1</sup> and A. Bermudez<sup>5</sup>

<sup>1</sup>*Johannes Gutenberg-Universität, Institut für Physik, Staudingerweg 7, 55099 Mainz, Germany*

<sup>2</sup>*MAINZ-Graduate School Materials Science in Mainz, Staudingerweg 9, 55099 Mainz, Germany*

<sup>3</sup>*ICFO-Institut de Ciències Fotoniques, The Barcelona Institute of Science and Technology,  
08860 Castelldefels (Barcelona), Spain*

<sup>4</sup>*ICREA, Lluís Companys 23, 08010 Barcelona, Spain*

<sup>5</sup>*Department of Physics, Swansea University, Singleton Park, Swansea SA2 8PP, United Kingdom  
and Instituto de Física Fundamental, IFF-CSIC, Madrid E-28006, Spain*

(Received 21 December 2016; revised manuscript received 10 August 2017; published 27 September 2017)

Understanding the robustness of topological phases of matter in the presence of strong interactions and synthesizing novel strongly correlated topological materials lie among the most important and difficult challenges of modern theoretical and experimental physics. In this work, we present a complete theoretical analysis of the synthetic Creutz-Hubbard ladder, which is a paradigmatic model that provides a neat playground to address these challenges. We give special attention to the competition of correlated topological phases and orbital quantum magnetism in the regime of strong interactions. These results are, furthermore, confirmed and extended by extensive numerical simulations. Moreover, we propose how to experimentally realize this model in a synthetic ladder made of two internal states of ultracold fermionic atoms in a one-dimensional optical lattice. Our work paves the way towards quantum simulators of interacting topological insulators with cold atoms.

DOI: [10.1103/PhysRevX.7.031057](https://doi.org/10.1103/PhysRevX.7.031057)

Subject Areas: Atomic and Molecular Physics,  
Quantum Information




# 2.3 The synthetic Creutz-Hubbard model

PHYSICAL REVIEW X **10**, 041007 (2020)

---

## Robust Topological Order in Fermionic $\mathbb{Z}_2$ Gauge Theories: From Aharonov-Bohm Instability to Soliton-Induced Deconfinement


Daniel González-Cuadra <sup>1,\*</sup> Luca Tagliacozzo,<sup>2</sup> Maciej Lewenstein,<sup>1,3</sup> and Alejandro Bermudez<sup>4</sup>

<sup>1</sup>*ICFO—Institut de Ciències Fotòniques, The Barcelona Institute of Science and Technology, Avinguda Carl Friedrich Gauss 3, 08860 Castelldefels (Barcelona), Spain*

<sup>2</sup>*Departament de Física Quàntica i Astrofísica and Institut de Ciències del Cosmos (ICCUB), Universitat de Barcelona, Martí i Franquès 1, 08028 Barcelona, Spain*

<sup>3</sup>*ICREA, Lluis Companys 23, 08010 Barcelona, Spain*

<sup>4</sup>*Departamento de Física Teórica, Universidad Complutense, 28040 Madrid, Spain*

 (Received 3 March 2020; revised 28 May 2020; accepted 14 August 2020; published 9 October 2020)

Topologically ordered phases of matter, although stable against local perturbations, are usually restricted to relatively small regions in phase diagrams. Thus, their preparation requires a precise fine-tuning of the system's parameters, a very challenging task in most experimental setups. In this work, we investigate a model of spinless fermions interacting with dynamical  $\mathbb{Z}_2$  gauge fields on a cross-linked ladder and show evidence of topological order throughout the full parameter space. In particular, we show how a magnetic flux is spontaneously generated through the ladder due to an Aharonov-Bohm instability, giving rise to topological order even in the absence of a plaquette term. Moreover, the latter coexists here with a symmetry-protected topological phase in the matter sector, which displays fractionalized gauge-matter edge states and intertwines with it by a flux-threading phenomenon. Finally, we unveil the robustness of these features through a gauge frustration mechanism, akin to geometric frustration in spin liquids, allowing topological order to survive to arbitrarily large quantum fluctuations. In particular, we show how, at finite chemical potential, topological solitons are created in the gauge field configuration, which bound to fermions and form  $\mathbb{Z}_2$  deconfined quasiparticles. The simplicity of the model makes it an ideal candidate for 2D gauge theory phenomena, as well as exotic topological effects, to be investigated using cold-atom quantum simulators.

DOI: [10.1103/PhysRevX.10.041007](https://doi.org/10.1103/PhysRevX.10.041007)

Subject Areas: Atomic and Molecular Physics,  
Condensed Matter Physics,  
Particles and Fields

## 2.3 The synthetic Creutz-Hubbard model

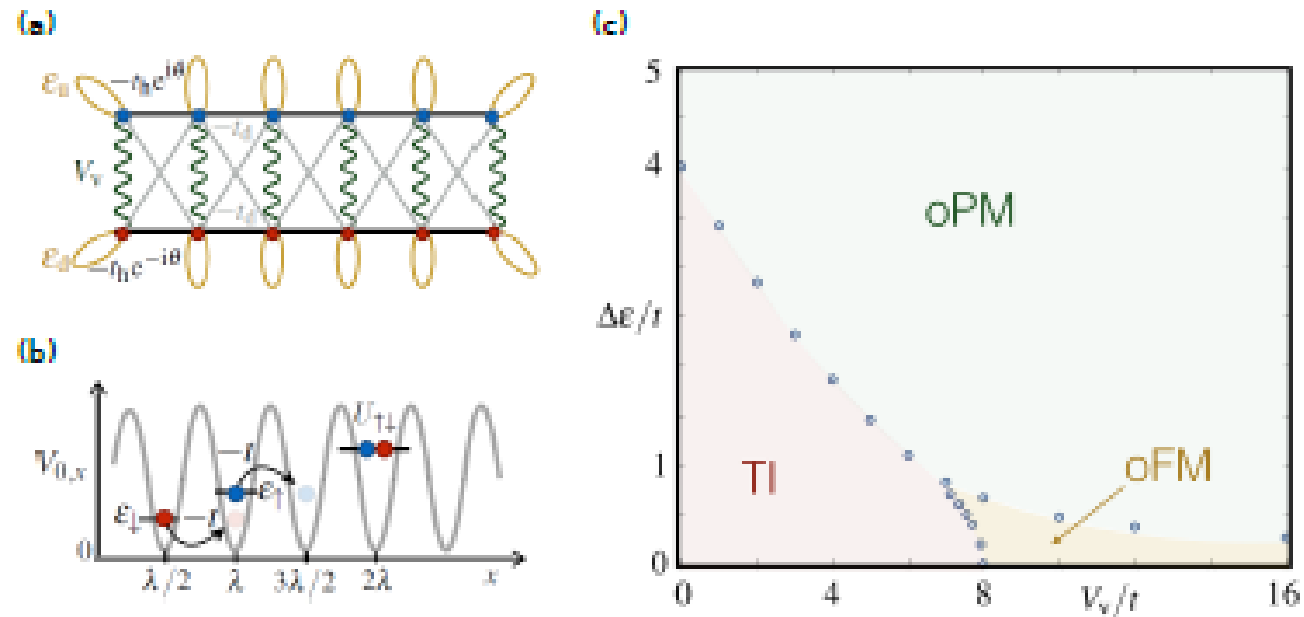


Figure 4. Creutz topological insulator: (a) The imbalanced Creutz ladder defined in Eq. (4.3) in the  $\pi$ -flux limit. (b) Atoms in two hyperfine states  $|\uparrow\rangle$ ,  $|\downarrow\rangle$  are trapped at the minima of an optical lattice. At low temperatures, the kinetic energy of the atoms can be described as a tunnelling of strength  $-t$  between the lowest energy levels  $\epsilon_{\uparrow}$ ,  $\epsilon_{\downarrow}$  of neighbouring potential wells. Additionally, the  $s$ -wave scattering of the atoms leads to contact interactions of strength  $U_{\uparrow\downarrow}$  whenever two fermionic atoms with different internal states meet on the same potential well. (c) Phase diagram of the C-H model. It displays a topological insulator phase (TI), and two other non-topological phases, namely an orbital phase with long-range ferromagnetic Ising order (oFM), and an orbital paramagnetic phase (oPM). The blue circles label numerical results and the coloured phase boundaries are a guide to the eye.

## 2.3 Wilson-Hubbard model

**Wilson-Hubbard model:** In the thermodynamic limit, the rungs of the ladder play the role of the 1d Bravais lattice  $ja \rightarrow x \in \Lambda_l = aZ^d = \{x : x_i \in Z, \forall i = 1, \dots, d\}$ , while the ladder index  $l \in \{u, d\}$  plays the role of the spinor degrees of freedom of the Fermi field  $\Psi(x) = (c_{j,u}, c_{j,d})^t$ . Making a gauge transformation  $c_{j,l} \rightarrow e^{i\pi j/2} c_{j,l}$ , one finds that the above imbalanced Creutz model (4.1) can be rewritten as a *1D Wilson-fermion Hamiltonian* lattice field theory (LFT). In

general the Wilson LFT is defined by the following Hamiltonian

$$\begin{aligned} \mathcal{H}_W = \sum_{x \in \Lambda_l} & \left[ \Psi^\dagger(x) \left( \frac{i\alpha_i}{2} + \frac{\delta m_i \beta}{2} \right) \Psi(x + au^i) + m \Psi^\dagger(x) \frac{\beta}{2} \Psi(x) + H.c. \right] \\ & + \sum_{\nu \mu} \sum_{x \in \Lambda_l} \Psi_\mu^\dagger(x) \Psi_\nu^\dagger(x) \frac{u_{\mu\nu}}{2} \Psi_\mu(x) \Psi_\nu(x) \end{aligned} \quad (4.5)$$

where the parameters  $\delta m_i$  quantify a certain mass shift introduced to put the fermion doublers up to the cut-off scale of the LFT, and  $u_{\mu,\nu} = (1 - \delta_{\mu,\nu})g^2$  encode the interaction strengths. In

## 2.3 Gross-Neveu model

**Gross-Neveu-Wilson model:** It is possible to map the imbalanced Creutz-Hubbard ladder to a discretized version of the Gross-Neveu field theory: the Gross-Neveu-Wilson field theory. This QFT describes Dirac fermions with  $N$  flavors interacting via quartic coupling which live in one spatial and one time dimension. In the continuum, the model is described by the following normal-ordered Hamiltonian  $H = \int dx : \mathcal{H} :$  with

$$\mathcal{H} = -\bar{\Psi}(x)i\gamma^1\partial_x\Psi(x) - \frac{g^2}{2N}(\bar{\Psi}(x)\Psi(x))^2. \quad (4.6)$$

Here  $\bar{\Psi}(x) = (\bar{\Psi}_1(x), \dots, \bar{\Psi}_N(x))$  where  $\bar{\Psi}_n(x) = \Psi_n^\dagger(x)\gamma^0$  are two-component spinor field operators for the  $n$ -th fermionic species, and  $\gamma^0 = \sigma^z, \gamma^1 = i\sigma^y$  are the gamma matrices, which can be expressed in terms of Pauli matrices for  $(1+1)$ -dimensional Minkowski space-time, leading to the chiral matrix  $\gamma^5 = \gamma^0\gamma^1 = \sigma^x$ . Therefore, the Gross-Neveu model describes a collection of  $N$  copies of massless Dirac field coupled via quartic interactions. According to the above discussion and using the exact relations  $ma = \frac{\Delta\epsilon}{4t} - 1$  and  $g^2 = \frac{V_v}{2t}$ , the Wilsonian discretization of the Gross-Neveu QFT on a uniform lattice (defined in Eq. 4.5) is gauge-equivalent to the imbalanced Creutz-Hubbard model of condensed-matter physics [71]. Fig. 5(a) shows the phase

## 2.3 Gross-Neveu model

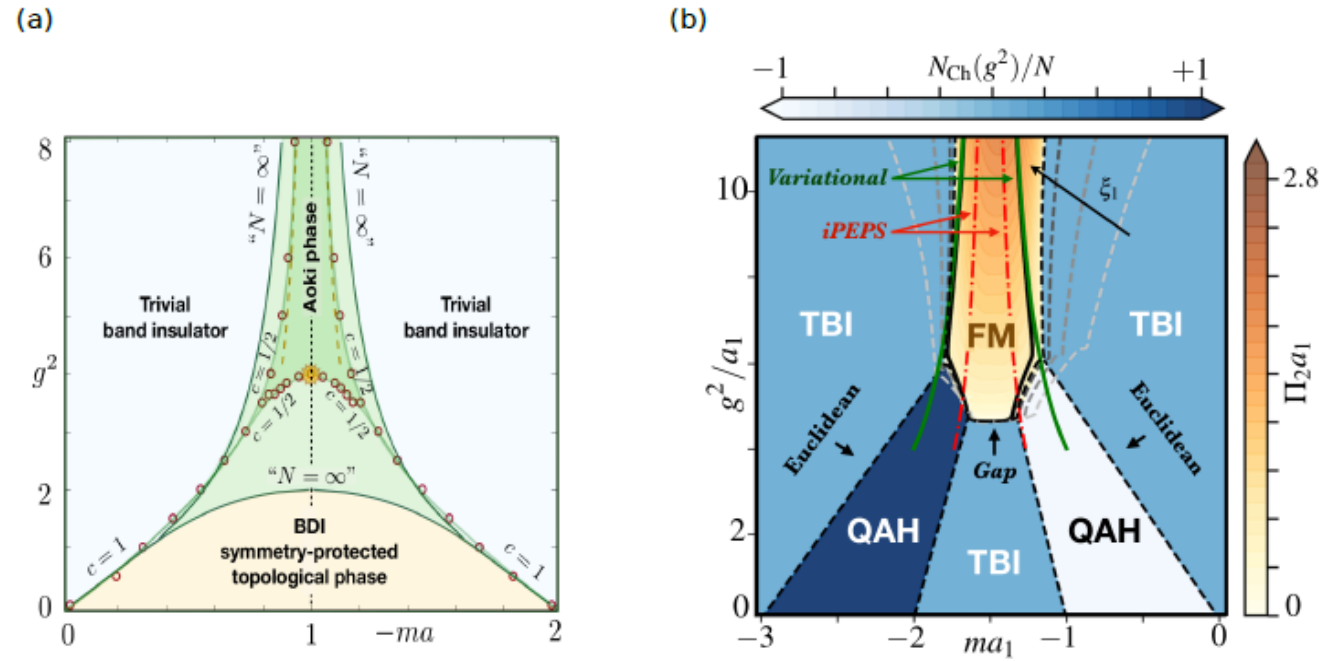




**Figure 5. Gross-Neveu model phase diagrams:** (a) Phase diagram of  $(1 + 1)d$  Gross-Neveu model. The two green solid lines correspond to the critical lines found by large- $N$  techniques. Red circles represent the critical points of the  $N = 1$  Gross Neveu lattice model obtained with MPS. The semi-transparent green lines joining these points delimit the trivial band insulator, Aoki phase, and the BDI symmetry-protected topological phase. We also include the exact critical point at  $(-ma, g^2) = (1, 4)$ , which is depicted by an orange star, and the strong-coupling critical lines that become exact in the limit of  $g^2 \rightarrow \infty$ , depicted by dashed orange lines. MPS predictions match these exact results remarkably well. (b) Phase diagram of  $(2 + 1)d$  Gross-Neveu model. Contour plots of the Chern number  $N_{Ch}$  (blue) and  $\pi$  condensate (orange), predicting large- $N$  QAH phases, trivial band insulators (TBIs), and a ferromagnetic phase (FM). The black solid line is obtained by solving self-consistent equations (*Gap*), which can delimit the area of the FM, but give no further information about the TBI or QAH phases. The green solid lines (*Variational*) represent the product-state prediction for the compass model, and the red dashed-dotted lines correspond to iPEPs.

### 3. Experimental and experimentally friendly quantum simulators

## 3.3 a) Density dependent gauge fields

# Realization of density-dependent Peierls phases to engineer quantized gauge fields coupled to ultracold matter

Frederik Görg, Kilian Sandholzer, Joaquín Minguzzi, Rémi Desbuquois , Michael Messer and Tilman Esslinger \*

Gauge fields that appear in models of high-energy and condensed-matter physics are dynamical quantum degrees of freedom due to their coupling to matter fields. Since the dynamics of these strongly correlated systems is hard to compute, it was proposed to implement this basic coupling mechanism in quantum simulation platforms with the ultimate goal to emulate lattice gauge theories. Here, we realize the fundamental ingredient for a density-dependent gauge field acting on ultracold fermions in an optical lattice by engineering non-trivial Peierls phases that depend on the site occupations. We propose and implement a Floquet scheme that relies on breaking time-reversal symmetry by driving the lattice simultaneously at two frequencies that are resonant with the on-site interactions. This induces density-assisted tunnelling processes that are controllable in amplitude and phase. We demonstrate techniques in a Hubbard dimer to quantify the amplitude and to directly measure the Peierls phase with respect to the single-particle hopping. The tunnel coupling features two distinct regimes as a function of the modulation amplitudes, which can be characterized by a  $\mathbb{Z}_2$ -invariant. Moreover, we provide a full tomography of the winding structure of the Peierls phase around a Dirac point that appears in the driving parameter space.

## 3.3 b) Floquet engineering of $\mathbb{Z}_2$ gauge fields

ARTICLES

<https://doi.org/10.1038/s41567-019-0649-7>

nature  
physics

# Floquet approach to $\mathbb{Z}_2$ lattice gauge theories with ultracold atoms in optical lattices

Christian Schweizer<sup>1,2,3</sup>, Fabian Grusdt<sup>3,4</sup>, Moritz Berngruber<sup>1,3</sup>, Luca Barbiero<sup>5</sup>, Eugene Demler<sup>6</sup>, Nathan Goldman<sup>5</sup>, Immanuel Bloch<sup>1,2,3</sup> and Monika Aidelsburger<sup>1,2,3\*</sup>

Quantum simulation has the potential to investigate gauge theories in strongly interacting regimes, which are currently inaccessible through conventional numerical techniques. Here, we take a first step in this direction by implementing a Floquet-based method for studying  $\mathbb{Z}_2$  lattice gauge theories using two-component ultracold atoms in a double-well potential. For resonant periodic driving at the on-site interaction strength and an appropriate choice of the modulation parameters, the effective Floquet Hamiltonian exhibits  $\mathbb{Z}_2$  symmetry. We study the dynamics of the system for different initial states and critically contrast the observed evolution with a theoretical analysis of the full time-dependent Hamiltonian of the periodically driven lattice model. We reveal challenges that arise due to symmetry-breaking terms and outline potential pathways to overcome these limitations. Our results provide important insights for future studies of lattice gauge theories based on Floquet techniques.



## 3.3 c) Local U(1) symmetry from spin-changing collisions

RESEARCH

---

QUANTUM SIMULATION

### A scalable realization of local U(1) gauge invariance in cold atomic mixtures

Alexander Mil<sup>1\*</sup>, Torsten V. Zache<sup>2</sup>, Apoorva Hegde<sup>1</sup>, Andy Xia<sup>1</sup>, Rohit P. Bhatt<sup>1</sup>, Markus K. Oberthaler<sup>1</sup>, Philipp Hauke<sup>1,2,3</sup>, Jürgen Berges<sup>2</sup>, Fred Jendrzejewski<sup>1</sup>

In the fundamental laws of physics, gauge fields mediate the interaction between charged particles. An example is the quantum theory of electrons interacting with the electromagnetic field, based on U(1) gauge symmetry. Solving such gauge theories is in general a hard problem for classical computational techniques. Although quantum computers suggest a way forward, large-scale digital quantum devices for complex simulations are difficult to build. We propose a scalable analog quantum simulator of a U(1) gauge theory in one spatial dimension. Using interspecies spin-changing collisions in an atomic mixture, we achieve gauge-invariant interactions between matter and gauge fields with spin- and species-independent trapping potentials. We experimentally realize the elementary building block as a key step toward a platform for quantum simulations of continuous gauge theories.

# 3.3 d) Minimal $SU(2)$ models for ultracold atom systems

IOP Publishing

New J. Phys. 22 (2020) 103027

<https://doi.org/10.1088/1367-2630/abb961>

**New Journal of Physics**

The open access journal at the forefront of physics

Deutsche Physikalische Gesellschaft  DPG  
IOP Institute of Physics

Published in partnership  
with: Deutsche Physikalische  
Gesellschaft and the Institute  
of Physics



OPEN ACCESS

RECEIVED  
18 June 2020

REVISED  
20 August 2020

ACCEPTED FOR PUBLICATION  
17 September 2020

PUBLISHED  
13 October 2020

Original content from  
this work may be used  
under the terms of the  
[Creative Commons  
Attribution 4.0 licence](#).

Any further distribution  
of this work must  
maintain attribution to  
the author(s) and the  
title of the work, journal  
citation and DOI.



PAPER

## From the Jaynes–Cummings model to non-abelian gauge theories: a guided tour for the quantum engineer

Valentin Kasper<sup>1,2,\*</sup>, Gediminas Juzeliūnas<sup>3</sup>, Maciej Lewenstein<sup>1,4</sup>, Fred Jendrzejewski<sup>5</sup>  
and Erez Zohar<sup>6</sup>

<sup>1</sup> ICFO-Institut de Ciències Fotoniques, The Barcelona Institute of Science and Technology, Av. Carl Friedrich Gauss 3, 08860 Castelldefels (Barcelona), Spain

<sup>2</sup> Department of Physics, Harvard University, Cambridge, MA, 02138, United States of America

<sup>3</sup> Institute of Theoretical Physics and Astronomy, Vilnius University, Saulėtekio 3, 10257 Vilnius, Lithuania

<sup>4</sup> ICREA, Pg. Lluís Companys 23, 08010 Barcelona, Spain

<sup>5</sup> Kirchhoff-Institut für Physik, Im Neuenheimer Feld 227, 69120 Heidelberg, Germany

<sup>6</sup> Racah Institute of Physics, The Hebrew University of Jerusalem, Givat Ram, Jerusalem 91904, Israel

\* Author to whom any correspondence should be addressed.

E-mail: [valentin.kasper@icfo.eu](mailto:valentin.kasper@icfo.eu)

Keywords: lattice gauge theory, quantum simulation, quantum optics

### Abstract

The design of quantum many body systems, which have to fulfill an extensive number of constraints, appears as a formidable challenge within the field of quantum simulation. Lattice gauge theories are a particular important class of quantum systems with an extensive number of local constraints and play a central role in high energy physics, condensed matter and quantum information. Whereas recent experimental progress points towards the feasibility of large-scale quantum simulation of abelian gauge theories, the quantum simulation of non-abelian gauge theories appears still elusive. In this paper we present minimal non-abelian lattice gauge theories, whereby we introduce the necessary formalism in well-known abelian gauge theories, such as the Jaynes–Cummings model. In particular, we show that certain minimal non-abelian lattice gauge theories can be mapped to three or four level systems, for which the design of a quantum simulator is standard with current technologies. Further we give an upper bound for the Hilbert space dimension of a one dimensional  $SU(2)$  lattice gauge theory, and argue that the implementation with current digital quantum computer appears feasible.

# 3.3 e) Non-Abelian gauge invariance from dynamical decoupling

## Local gauge invariance from dynamical decoupling

Valentin Kasper,<sup>1,2</sup> Torsten Zache,<sup>3</sup> Fred Jendrzejewski,<sup>3</sup> Maciej Lewenstein,<sup>1,4</sup> and Erez Zohar<sup>5</sup>

<sup>1</sup>*ICFO - Institut de Ciències Fotoniques, The Barcelona Institute of Science and Technology,  
Av. Carl Friedrich Gauss 3, 08860 Castelldefels (Barcelona), Spain*

<sup>2</sup>*Department of Physics, Harvard University, Cambridge, MA, 02138, USA\**

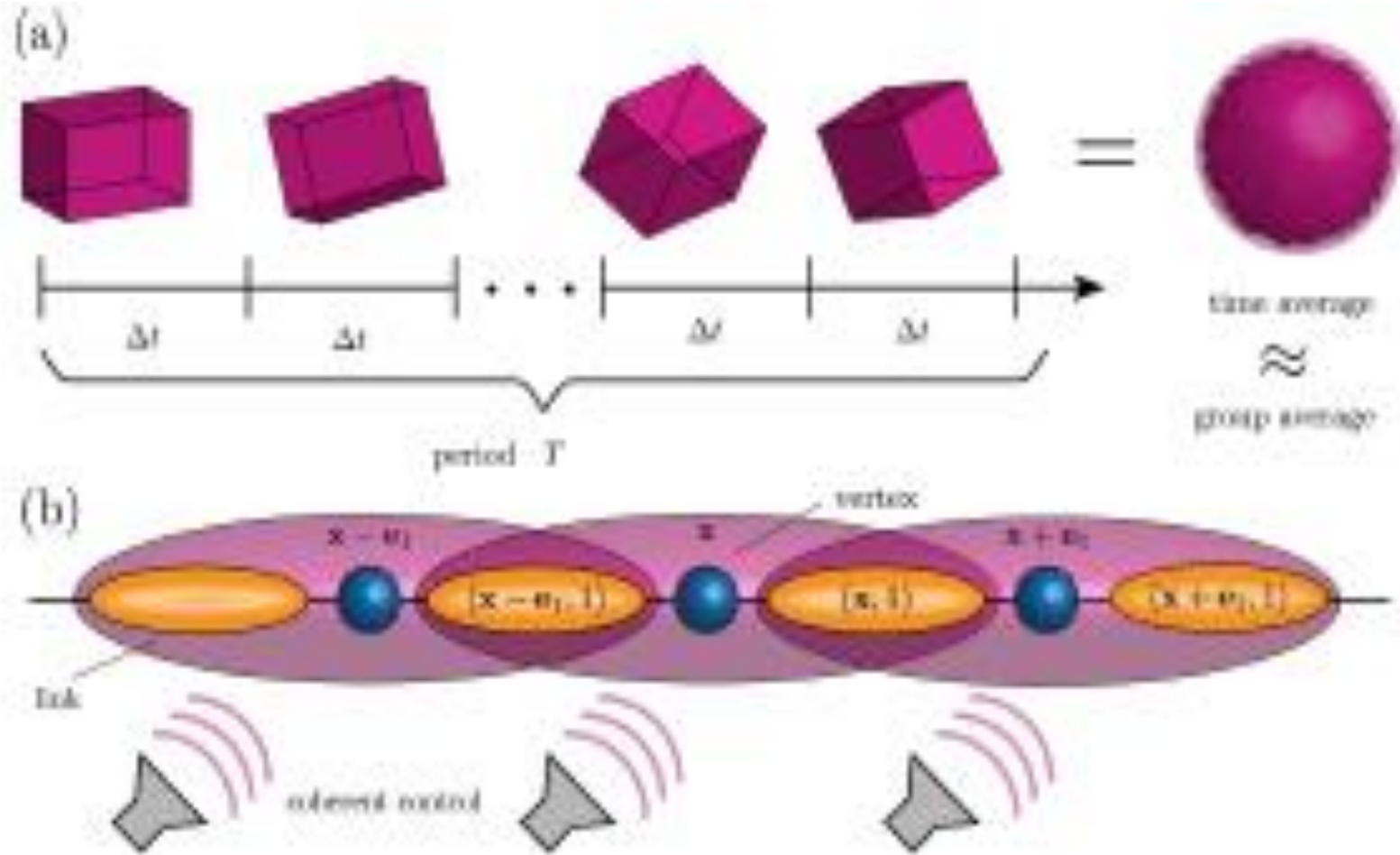
<sup>3</sup>*Heidelberg University, Institut fuer Theoretische Physik,  
Philosophenweg 16, D-69120 Heidelberg, Germany*

<sup>4</sup>*ICREA, Pg. Lluís Companys 23, 08010 Barcelona, Spain*

<sup>5</sup>*Racah Institute of Physics, The Hebrew University of Jerusalem, Givat Ram, Jerusalem 91904, Israel  
(Dated: December 1, 2020)*

Lattice gauge theories are fundamental to such distinct fields as particle physics, condensed matter and quantum information theory. Recent progress in the control of artificial quantum systems allows for studying Abelian lattice gauge theories in table-top experiments, however, the realization of non-Abelian models remains challenging. Here, we employ a coherent quantum control scheme to enforce non-Abelian local gauge invariance on a quantum simulator. We illustrate this idea in detail for a one dimensional lattice system to engineer  $SU(2)$  local gauge invariance. We then comment on how to apply this scheme to other non-Abelian gauge symmetries and higher dimensions opening up an alternative direction for the quantum simulation of non-Abelian lattice gauge theories.

### 3.3 e) Non-Abelian gauge invariance from dynamical decoupling



### 3.3 e) Non-Abelian gauge invariance from dynamical decoupling

Consider a lattice Hamiltonian  $\tilde{H} = H_0 + H_1(t)$ , where  $H$  acts on a Hilbert space with particles on the vertices  $\mathbf{x}$  and particles on the links  $(\mathbf{x}, i)$ , where the link starts at  $\mathbf{x}$  and points towards  $i$  (see Fig. 1). Explain  $H_0$ . The time independent part is denoted by  $H_0$  and the coherent drive with period  $T$  is  $H_1(t) = H_1(t + T)$ . For a strong, coherent, and periodic drive  $H_1$ , the time evolution is given by effective Hamiltonian of the many body systems is given by

$$\bar{H}_0 \equiv \frac{1}{T} \int_0^T ds U_1^\dagger(s) H_0 U_1(s), \quad (1)$$

which is obtained from the first order Magnus expansion [32–34] after going to the interaction picture with  $U_1(t)$ . In particular, the unitary  $U_1(t)$  is generated by the periodic drive  $H_1(t)$  and we ask how to choose the periodic drive  $H_1(t)$  to render the effective Hamiltonian local gauge invariant.

### 3.3 e) Non-Abelian gauge invariance from dynamical decoupling

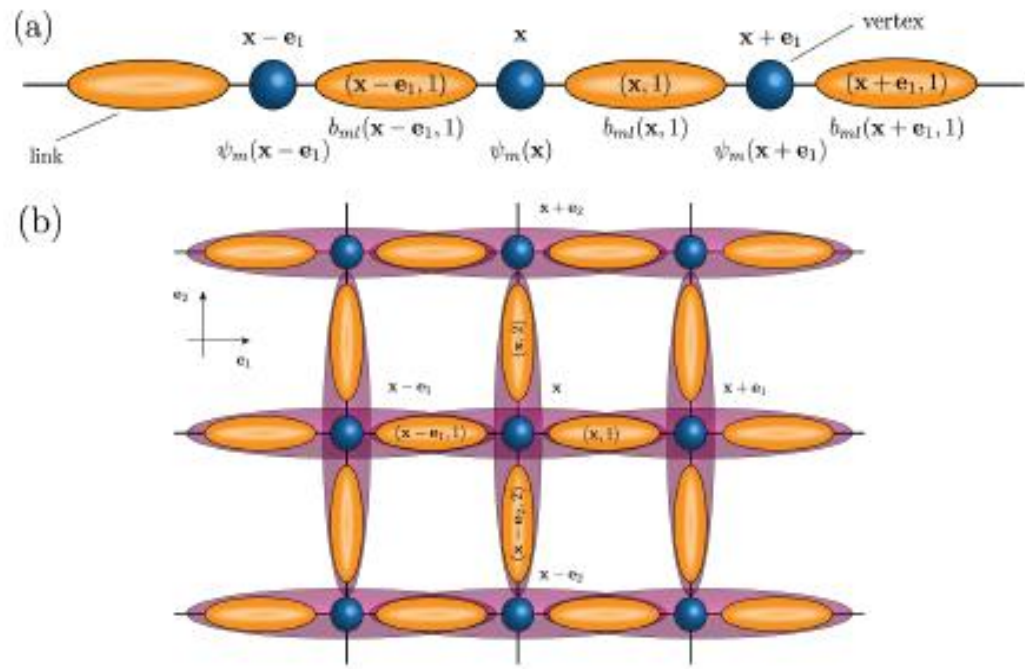


FIG. 2. **One/two dimensional lattice gauge theory:** (a) Fermions on the vertices and bosons on the links. (b) The green, purple and red bubbles indicate the coherent drive. Assuming only overlap between neighboring objects one needs three independent, but global coherent driving fields in order to enforce local gauge invariance.

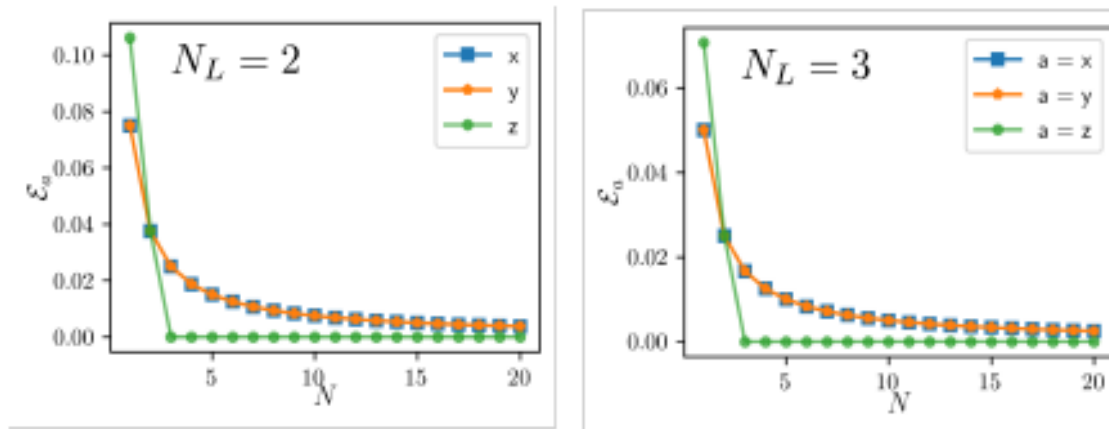


FIG. 3. **Error reduction:**

The error measure introduced in Eq. (??) reduces the violation of local gauge invariance. With increasing  $N$  periodic drive samples more points of the SU(2) manifold and hence reduces the error. We show the procedure for

## 3.3 f) Rotor Jackiw-Rebbi model

PRX QUANTUM 1, 020321 (2020)

---

### Rotor Jackiw-Rebbi Model: A Cold-Atom Approach to Chiral Symmetry Restoration and Charge Confinement

D. González-Cuadra<sup>1,\*</sup>, A. Dauphin<sup>1</sup>, M. Aidelsburger<sup>2,3</sup>, M. Lewenstein<sup>1,4</sup> and A. Bermudez<sup>5</sup>

<sup>1</sup>*ICFO - Institut de Ciències Fotòniques, The Barcelona Institute of Science and Technology, Av. Carl Friedrich Gauss 3, Castelldefels (Barcelona) 08860, Spain*

<sup>2</sup>*Fakultät für Physik, Ludwig-Maximilians-Universität, Schellingstr. 4, München D-80799, Germany*

<sup>3</sup>*Munich Center for Quantum Science and Technology (MCQST), Schellingstr. 4, München D-80799, Germany*

<sup>4</sup>*ICREA, Lluís Companys, 23, Barcelona 08010, Spain*

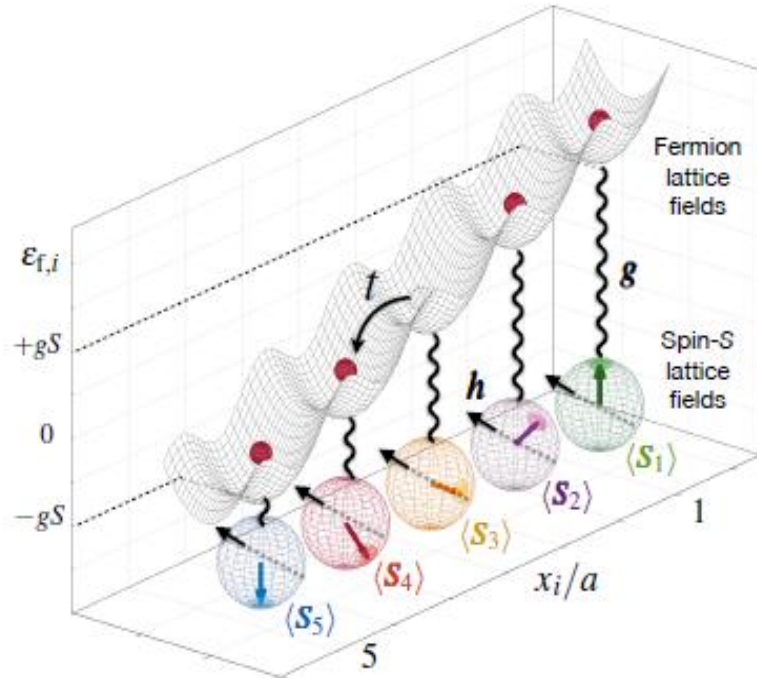
<sup>5</sup>*Departamento de Física Teórica, Universidad Complutense, Madrid 28040, Spain*



(Received 24 August 2020; accepted 20 November 2020; published 16 December 2020)

Understanding the nature of confinement, as well as its relation with the spontaneous breaking of chiral symmetry, remains one of the long-standing questions in high-energy physics. The difficulty of this task stems from the limitations of current analytical and numerical techniques to address nonperturbative phenomena in non-Abelian gauge theories. In this work, we show how similar phenomena emerge in simpler models, and how these can be further investigated using state-of-the-art cold-atom quantum simulators. More specifically, we introduce the rotor Jackiw-Rebbi model, a  $(1 + 1)$ -dimensional quantum field theory where interactions between Dirac fermions are mediated by quantum rotors. Starting from a mixture of ultracold atoms in an optical lattice, we show how this quantum field theory emerges in the long-wavelength limit. For a wide and experimentally relevant parameter regime, the Dirac fermions acquire a dynamical mass via the spontaneous breakdown of chiral symmetry. We study the effect of both quantum and thermal fluctuations, and show how they lead to the phenomenon of chiral symmetry restoration. Moreover, we uncover a confinement-deconfinement quantum phase transition, where mesonlike fermions fractionalize into quarklike quasiparticles bound to topological solitons of the rotor field. The proliferation of these solitons at finite chemical potentials again serves to restore the chiral symmetry, yielding a clear analogy with the quark-gluon plasma in quantum chromodynamics, where the restored symmetry coexists with the deconfined fractional charges. Our results indicate how the interplay between these phenomena could be analyzed in more detail in realistic atomic experiments.

### 3.3 f) Rotor Jackiw-Rebbi model



$$H = \sum_i \left( -t \left( c_i^\dagger c_{i+1} + c_{i+1}^\dagger c_i \right) + \mathbf{g} \cdot \mathbf{S}_i c_i^\dagger c_i - \mathbf{h} \cdot \mathbf{S}_i \right). \quad (1)$$

FIG. 1. **Discretised rotor Jackiw-Rebbi model:** Fermions tunnel with strength  $t$  against an energy landscape set by the lattice spins  $\varepsilon_{f,i} = \mathbf{g} \cdot \langle \mathbf{S}_i \rangle$ , which additionally precess under a magnetic field  $\mathbf{h}$ . In the figure, we show a possible configuration of the spins that lead to an energy landscape with a simple gradient. In the text, we show that other configurations that break translational symmetry appear directly in the equilibrium states of the model.



### 3.3 f) Rotor Jackiw-Rebbi model

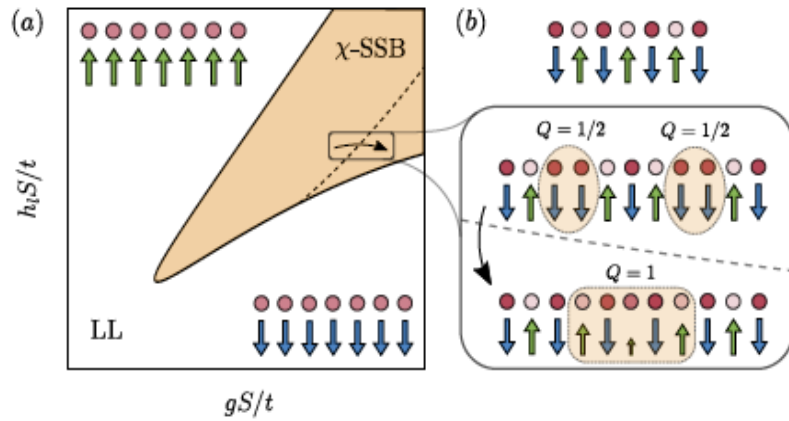


FIG. 2. **Phase diagram of the rotor Jackiw-Rebbi model:** (a) In the figure, we represent qualitatively the different phases that appear in the half-filled vacuum in terms of the interaction  $g$  and the longitudinal field  $h_\ell$ , for fixed values of the transverse field  $h_\tau$  and temperature  $T$ . Chiral symmetry is spontaneously broken in the shaded region ( $\chi$ -SSB), where the fermions develop a dynamical mass and the spins display Néel long-range order, as depicted in the upper panel of (b). This region is surrounded by a chiral-symmetric phase with a longitudinal paramagnet for the spins, such that the interacting massless fermions form a Luttinger liquid (LL). (b) Within the ordered region, we find two different quasi-particle regimes, separated in the figure by a dashed line. In the first one, deconfined topological defects in the spins bound repulsive quark-like fermions with fractional charges. In the second one, the quasi-particles attract each other, forming meson-like fermion bags with integer charge. For a finite doping density, the two regimes are separated by a first-order confinement-deconfinement phase transition, which coincides with a chiral symmetry restoration due to the proliferation of defects.

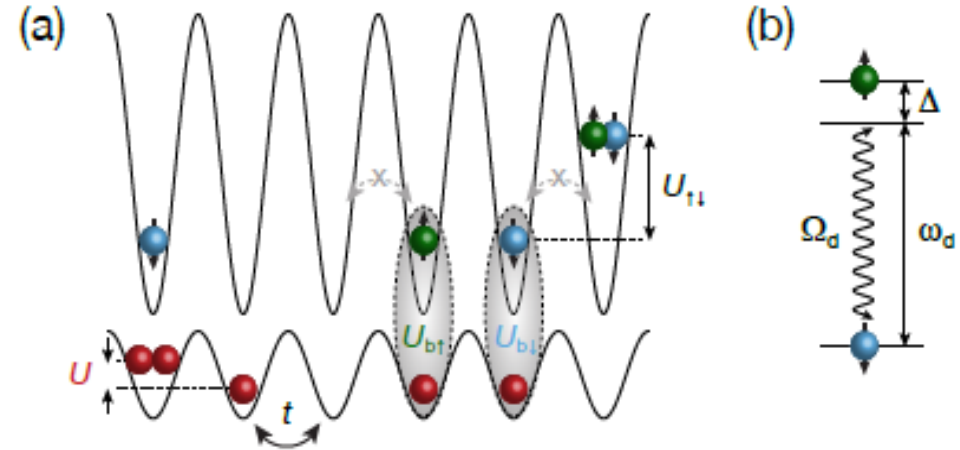


FIG. 3. **Bose-Fermi quantum simulator:** (a) Optical lattice potentials for both the bosonic atoms, here represented by red spheres, and the two-state fermionic atoms, here represented by green (blue) spheres for the  $\uparrow$  ( $\downarrow$ ) states. The bosons have a tunnelling amplitude  $t$ , and the Bose-Hubbard on-site interaction  $U$ . Conversely, the fermionic tunnelling is suppressed by the very deep lattice, and the Fermi-Hubbard on-site interaction strength is  $U_{\uparrow\downarrow}$ . When residing on the same lattice site, bosons and fermions interact with different strengths  $U_{b\uparrow} \neq U_{b\downarrow}$ . (b) Driving that induces Rabi oscillations between the fermionic states with Rabi frequency  $\Omega_d$  and detuning  $\Delta_d$ .

### 3.3 f) Rotor Jackiw-Rebbi model

$$\begin{aligned}
 H_m = & -t \sum_i \left( \hat{b}_i^\dagger \hat{b}_{i+1} + \text{H.c.} \right) + \frac{U}{2} \sum_i \hat{b}_i^\dagger \hat{b}_i^\dagger \hat{b}_i \hat{b}_i - \sum_i \mu_i \hat{b}_i^\dagger \hat{b}_i \\
 & + \sum_i \left( U_{\uparrow\downarrow} \hat{f}_{i\uparrow}^\dagger \hat{f}_{i\downarrow}^\dagger \hat{f}_{i\downarrow} \hat{f}_{i\uparrow} + \sum_\sigma U_{b\sigma} \hat{f}_{i\sigma}^\dagger \hat{f}_{i\sigma} \hat{b}_i^\dagger \hat{b}_i \right) - \sum_{i,\sigma} \mu_{i,\sigma} \hat{f}_{i\sigma}^\dagger \hat{f}_{i\sigma}.
 \end{aligned} \tag{2}$$

Here,  $\mu_i$  ( $\mu_{i,\sigma}$ ) is the local chemical potential for the bosons (fermions),  $U$  ( $U_{\uparrow\downarrow}$ ) is the on-site Hubbard interaction due to  $s$ -wave collisions between a pair of bosons (fermions), and  $U_{b\uparrow}, U_{b\downarrow}$  stem from the corresponding fermion-boson scattering. In addition, the Hamiltonian for the internal degrees of freedom of the fermionic atoms reads

$$H_{\text{int}} = \sum_i \left( \sum_\sigma \frac{\varepsilon_\sigma}{2} \hat{f}_{i\sigma}^\dagger \hat{f}_{i\sigma} + \frac{\Omega_d}{2} e^{-i\omega_d t} \hat{f}_{i\uparrow}^\dagger \hat{f}_{i\downarrow} + \text{H.c.} \right), \tag{3}$$

$$\mathcal{H} = \bar{\Psi}(x) \left( -ic\gamma^1 \partial_1 + \mathbf{g}_s \cdot \mathbf{n}(x) \right) \Psi(x) + (\mathbf{g} j_0(x) - \mathbf{h}) \cdot \boldsymbol{\ell}(x), \tag{6}$$

where  $\bar{\Psi}(x) = \Psi^\dagger(x)\gamma^0$  is the adjoint for the spinor  $\Psi(x) = (\psi_+(x), \psi_-(x))^t$ , the gamma matrices are  $\gamma^0 = \sigma^x$ ,  $\gamma^1 = -i\sigma^y$ , and the charge-density is  $j_0(x) = \bar{\Psi}(x)\gamma_0\Psi(x)$ . Additionally, we have introduced the coupling  $\mathbf{g}_s = gS\mathbf{e}_z$ , and  $\partial_1 = \partial/\partial x$ .

### 3.3 f) Rotor Jackiw-Rebbi model

7

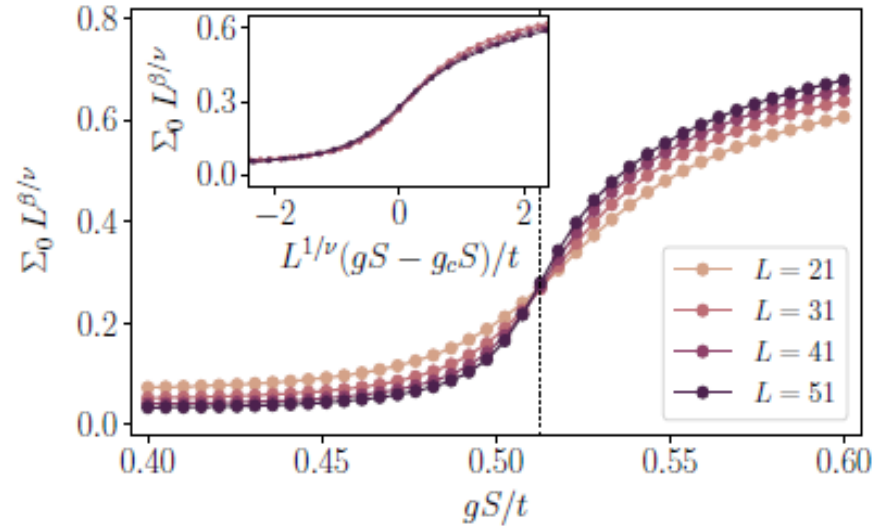


FIG. 5. **Scalar condensate and chiral SSB:** We represent the scalar fermion condensate  $\Sigma_0 = \langle \bar{\Psi}\Psi \rangle$  in terms of  $gS/t$  for the ground state of a half-filled chain of different lengths  $N_s$ , with  $h_\ell S = 0.3t$  and  $h_t S = 0.05t$ . The results are obtained using DMRG for  $S = 1/2$ . Using the critical exponents of the 2D Ising universality class ( $\nu = 1$ ,  $\beta = 1/8$ ), the lines cross at the critical point obtained for the infinite system with iDMRG, and collapse for an appropriate rescaling (inset).

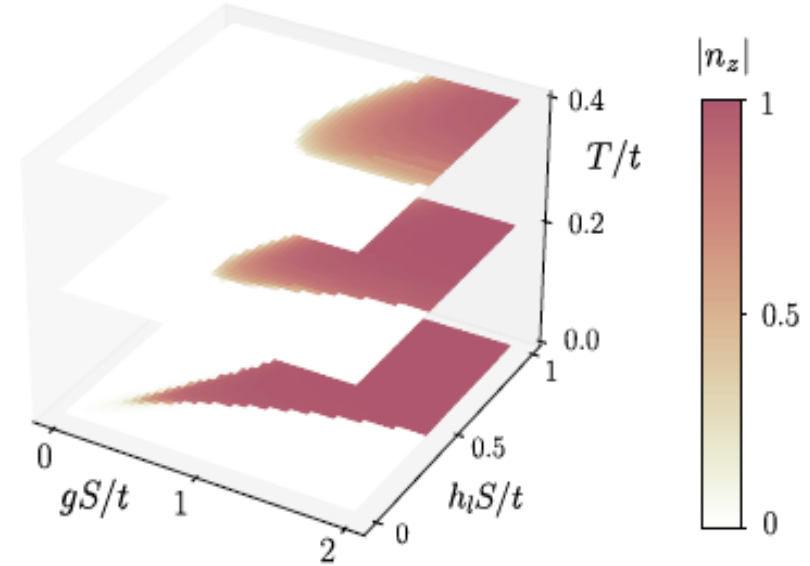


FIG. 6. **Chiral symmetry restoration at finite temperatures:** Phase diagram for different  $T/t$  and  $h_t S = 0.05t$ , where we represent the Néel order parameter  $n_z$  calculated in the HF approximation. The AF phase, where chiral symmetry is spontaneously broken, shrinks as the temperature increases. In the high-energy-physics lore, one says that chiral symmetry is restored at high temperatures.

## 4. Outlook: Experiments?

## Conclusions

Enjoy physics and beyond!!!

# Quantum Narcissism

The Amateur's Guide to Avantgarde:  
Catalunya, Poland, Portugal, and  
More...



Maciej Lewenstein<sup>1</sup>

April 19, 2021

<sup>1</sup>©Maciej Lewenstein 2015

<https://theamateursguidetoavantgarde.bandcamp.com/album/the-amateurs-guide-to-avantgarde>